

**A STUDY OF LEAD AND CHROMIUM ADSORPTION USING CARBON
NANOMATERIALS**

by

Nor Alwani Binti Abd Ghani @ Yaacob

Dissertation submitted in partial fulfillment of
the requirements for the
Bachelor of Engineering (Hons)
(Chemical Engineering)

SEPTEMBER 2011

Universiti Teknologi PETRONAS
Bandar Seri Iskandar
31750 Tronoh
Perak Darul Ridzuan

CERTIFICATION OF APPROVAL

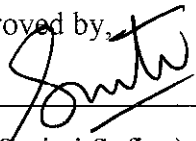
A Study of Lead and Chromium Adsorption using Carbon Nanomaterials

By

Nor Alwani Binti Abd Ghani @ Yaacob

A project dissertation submitted to the
Chemical Engineering Programme
Universiti Teknologi PETRONAS
in partial fulfillment of the requirement for the
BACHELOR OF ENGINEERING (Hons)
(CHEMICAL ENGINEERING)

Approved by,

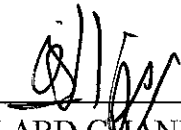


(Dr. Suriati Sufian)

UNIVERSITI TEKNOLOGI PETRONAS
TRONOH, PERAK
| SEPTEMBER 2011

CERTIFICATION OF ORIGINALITY

This is to verify that I am responsible for the work submitted in this project, that the original work is own my own except as specified in the references and acknowledgement, that the original work contained herein have not been undertaken or done by unspecified sources of persons



(NOR ALWANI BINTI ABD GHANI @ YAACOB)

ACKNOWLEDGEMENT

It is a pleasure to thank those who made this final year project (FYP) possible, I would like to take this opportunity to thank and acknowledge all parties who played role in making my FYP successful.

Deepest regards are dedicated to my supervisor, Dr. Suriati Sufian for her endless and priceless guidance and support throughout of the FYP period. Special thanks go to Nurul Syafiqin Mohamad Shah who has been supportively helping me throughout of the FYP period. Without them, the project would be impossible to be done.

Not to forget, Dr. Lukman Ismail as the FYP coordinator who has been helping me in completing the FYP. Thank you for your help throughout of the project. Besides, I would like to thank Universiti Teknologi PETRONAS (UTP) for providing the lab facilities in order to make this FYP possible. I owe my deepest gratitude to all the technicians, those who helped me throughout of her FYP period. Without them, this project would be difficult to be completed.

Lastly, I would like to convey my gratitude to my family members especially my mother – Esah Abdullah and my father – Abd Ghani @ Yaacob Mamat and to all my friends for their moral support throughout of the FYP period.

Thank you.

With deepest gratitude and appreciation,

.....


Nor Alwani Binti Abd Ghani @ Yaacob

Chemical Engineering Department

ABSTRACT

Rapid development of industries in the world has been the major contributor to pollution of water resources such as heavy metals. These heavy metals are very hazardous to both human and environment since they do not degrade into harmless end product but they eventually will be accumulated in living organisms and thus causing various illnesses and syndromes. Many methods have been researched in order to remove these dangerous heavy metals and one of the best methods is adsorption. Present study was undertaken to investigate ability of carbon nanotubes (CNTs) and carbon nanofibers (CNFs) as adsorbents in adsorption process of removing lead and chromium ions from aqueous solutions. The analyses of metal ions removal were performed on four operation parameters which were initial ion concentration, contact time, pH and temperature. The experiments were carried out using a bath shaker at constant speed of 200 rpm. BET surface area of CNFs was found to be 194.99 m²/g, while for CNTs, the BET surface area was found to be 478.99 m²/g. Batch adsorption test showed that adsorption of lead and chromium uptakes increase as the contact time increases till equilibrium. Besides, it was found that higher initial metal concentration resulted to better adsorption uptake till it reached its limit as the adsorbate per adsorbent ratio increased. Adsorption is optimum from pH 5 to 9 for chromium, while for lead, pH 6 and pH 9 are considered as optimum pH. Increased in temperature will slightly promote desorption of lead. However, it does not affect much on chromium adsorption. The equilibrium data fitted to Freundlich isotherm better for both metals in comparison with Langmuir isotherm, indicating that the adsorption processes are multilayer.

TABLE OF CONTENTS

ACKNOWLEDGEMENT	III
ABSTRACT	IV
TABLE OF CONTENTS	V
LIST OF FIGURES	VIII
LIST OF TABLES	XI
ABBREVIATIONS AND NOMENCLATURES	XII
1 CHAPTER 1 INTRODUCTION	1
1.1 BACKGROUND OF STUDY.....	1
1.2 PROBLEM STATEMENT.....	2
1.2.1 Problem identification	2
1.2.2 Significance of the project	2
1.3 AIM AND OBJECTIVES.....	3
1.3.1 Main aim	3
1.3.2 Specific objectives	3
1.3.3 Scope of study	3
1.4 RELEVANCY OF PROJECT	4
1.5 FEASIBILITY OF THE PROJECT	4
2 CHAPTER 2 LITERATURE REVIEW	5
2.1 FACTORS AFFECTING THE ADSORPTION PROCESS	5
2.1.1 Effect of contact time	5
2.1.2 Effect of initial metal concentration.....	6
2.1.3 Effect of pH	7
2.1.4 Effect of temperature.....	9
2.1.5 Effect of adsorbent dosage	10
2.1.6 Effect of agitation speed	11
2.1.7 Effect of functionalization.....	12

2.2 FUNCTIONALIZATION OF CARBON NANOFIBERS (CNFs)	13
2.2.1 Carbon Nanofibers and Carbon Nanotubes functionalization	13
2.2.2 Surface characterization techniques	16
2.2.3 Surface modification techniques	22
2.3 REVIEW REMARKS	26
3 CHAPTER 3 METHODOLOGY	27
3.1 PRELIMINARY RESEARCH ANALYSIS	27
3.2 LABORATORY WORK	27
3.3 EXPERIMENTAL METHODS	29
3.3.1 Experimental flow	29
3.3.2 BET surface area and pore size distribution testing	29
3.3.3 Batch adsorption studies	30
3.3.4 Metal solution preparation	31
3.3.5 Effect of contact time of metal adsorption	31
3.3.1 Effect of initial metal concentration on metal uptake	31
3.3.2 Effect of pH	32
3.3.3 Effect of temperature	32
3.3.4 Adsorption isotherms model	33
3.3.5 Metal concentration determination using AAS	33
3.4 GANTT CHART FOR THE FIRST SEMESTER OF FYP	34
3.5 GANTT CHART FOR THE SECOND SEMESTER OF FYP	35
4 CHAPTER 4 RESULTS AND DISCUSSION	36
4.1 BET SURFACE AREA CARBON NANOMATERIALS	36
4.2 PORE SIZE DISTRIBUTIONS	36
4.3 ADSORPTION ISOTHERM OF ADSORBENTS USING LIQUID NITROGEN	38
4.4 PRE-EXPERIMENTAL ANALYSIS	40
4.5 EFFECT OF CONTACT TIME ON METALS ADSORPTION	41
4.6 EFFECT OF INITIAL CONCENTRATION ON METALS ADSORPTION	42
4.7 EFFECT OF PH ON METALS ADSORPTION	44
4.8 EFFECT OF TEMPERATURES ON METALS UPTAKE	46

4.9 ADSORPTION ISOTHERM OF METALS ADSORPTION PROCESS	47
4.9.1 Langmuir isotherm	47
4.9.2 Freundlich Isotherm	48
5 CHAPTER 5 CONCLUSION AND RECOMMENDATION	49
5.1 CONCLUSION	49
5.2 RECOMMENDATIONS.....	49
5.2.1 Functionalization of carbon nanomaterials.....	49
5.2.2 Analysis on adsorbent used	49
5.2.3 Calibration of Atomic Absorption Spectrophotometer (AAS).....	50
REFERENCES	51
APPENDICES.....	54
APPENDIX A	54
APPENDIX B	59
APPENDIX C	60
APPENDIX D	61
APPENDIX E.....	62

LIST OF FIGURES

Figure 2-1: Effect of contact time on zinc removal using R-CNFs and M-CNFs at 150 rpm, pH 7 and 50mg (Atieh, 2011).....	5
Figure 2-2: Effect of initial Pb concentration on sorption capacity and removal (Ahmed et al., 2010).....	6
Figure 2-3: Effect of zinc concentration on percentage of removal of zinc at 150 rpm, pH 7 and 2 hr (Atieh, 2011).....	7
Figure 2-4: Effect of modified CNFs (M-CNFs) and raw CNFs (R-CNFs) on the removal of zinc at different pH (Atieh, 2011).....	8
Figure 2-5: Effect of pH on removal of Pb using CNFs (Ahmed et al., 2010).....	9
Figure 2-6: Langmuir isotherm of Zn(II) sorption by multiwalled carbon nanotubes (MWCNTs) at various temperature (Lu et al., 2006).....	10
Figure 2-7: Effect of CNFs' dosage on percentage of removal of zinc at 150 rpm, pH 7 and 2 hr (Atieh, 2011).....	11
Figure 2-8: Effect of agitation speed on percentage removal of zinc at pH 7 and 2 hr (Atieh, 2011).....	12
Figure 2-9: Schematic representation of a carbon nanofiber consisting of a multitude of small graphite layers separated at a distance of 0.35 nm (Rodriguez, 2000)....	13
Figure 2-10: A) defect-group functionalization, B) covalent sidewall functionalization, C) noncovalent functionalization with surfactants D) noncovalent functionalization with polymers and E) endohedral functionalization (Korneva, 2008).....	14
Figure 2-11: Schematic of carbon nanostructures a) single sheet of graphite, b) CNT consisting of concentric grapheme sheets, c) CNF composed of stacked grapheme cones at an angle alpha with respect to the axis of the fiber. The two primary CNFs structures: d) herringbone-type CNF and e) bamboo-type CNF f) vertically aligned CNF composed of a Ni catalyst nanoparticle at the tip and a graphitic fiber body (Klein et al., 2008).....	15
Figure 2-12: TEM of untreated (a) fishbone (herringbone) and (b) parallel (bamboo) CNFs with the corresponding IR spectroscopy results (Ros et al., 2002).....	17

Figure 2-13: SEM images of plasma treated CNFs (a) before and (b) after a 5 min growth of secondary nanofibers (Xia et al., 2005).....	19
Figure 2-14: STEM images and cartoons of the nanofiber outer wall structure [(a) and (b)] using a Ni catalyst and [(c) and (d)] using Pd catalyst. The white arrows in the STEM images points towards the catalyst particles at tip of the fiber (Ominami et al., 2005)	20
Figure 2-15: Schematic representation of the growth of (a) a CNF using conventional thermal CVD, (b) vertically aligned carbon nanostructure using PECVD, and (c) a carbon nanocone formed due to additional precipitation of C on the outer walls during PECVD (Klein et al., 2008).....	23
Figure 2-16: (a) Schematic illustration of the steps involved in the functionalization of CNFs and subsequent procedure for electroless deposition. (b) chemical transformations involved in the nanofiber modification (Klein et al., 2008)....	24
Figure 3-1: Adsorption process experimental flow	29
Figure 3-2: Surface area and pore size analyzer	30
Figure 3-3: Atomic adsorption spectrophotometer (AAS)	30
Figure 3-4: Bath shaker used in the adsorption process	32
Figure 3-5: Gantt chart for the first semester of final year project	34
Figure 3-6: Gantt chart for the second semester of final year project	35
Figure 4-1: Pore size distribution of carbon nanofibers (CNFs).....	36
Figure 4-2: Pore size distribution of carbon nanotubes (CNTs)	37
Figure 4-3: Adsorption isotherm of carbon nanofibers (CNFs).....	38
Figure 4-4: Adsorption isotherm for carbon nanotube (CNTs)	39
Figure 4-5: Comparison between CNFs and CNTs adsorbents on lead adsorption at different initial concentrations	40
Figure 4-6: Effect of contact time on lead adsorption at different initial metal concentrations using CNFs, at pH 6, adsorbent dosage of 1g/litre, 25°C and 200 rpm	41
Figure 4-7: Effect of contact time on chromium adsorption at different initial metal concentrations using CNFs, at pH 6, adsorbent dosage of 1g/litre, 25°C and 200 rpm	42

Figure 4-8: Effect of initial metal concentration on lead adsorption using CNFs, adsorbent dosage of 1g/litre, 25°C, pH 6 and 200 rpm	43
Figure 4-9: Effect of initial metal concentration on chromium adsorption using CNFs, adsorbent dosage of 1g/litre, 25°C, pH 6 and 200 rpm	44
Figure 4-10: Effect of solution's pH on lead adsorption using CNFs, at 25 ppm lead concentration, adsorbent dosage of 1g/litre, 25°C and 200 rpm	45
Figure 4-11: Effect of solution's pH on chromium adsorption using CNFs, at 25 ppm chromium concentration, adsorbent dosage of 1g/litre, 25°C and 200 rpm	45
Figure 4-12: Effect of temperature on lead and chromium adsorption using CNFs, at pH 6, adsorbent dosage of 1g/litre, 25 ppm and 200 rpm	46
Figure 4-14: Langmuir isotherm for chromium adsorption	47
Figure 4-15: Freundlich isotherm for chromium adsorption	48

LIST OF TABLES

Table 3-1: List of chemicals and adsorbent used.....	27
Table 3-2: Equipment/ tools required for experiment.....	28
Table 4-1: Classification of pore size (IUPAC)	37

ABBREVIATIONS AND NOMENCLATURES

AAS	: Atomic absorption spectrophotometer
AES	: Auger electron spectroscopy
AFM	: Atomic force microscopy
ALD	: Atomic layer deposition
As	: Arsenic
Å	: Angstrom
Ba	: Barium
BET	: Brunner-Emmet-Teller
C	: Carbon
Cd	: Cadmium
CNFs	: Carbon Nanofibers
cm ³ /g	: Centimeter cube per gram
CNTs	: Carbon Nanotubes
COOH	: Carboxylic functional group
Cr	: Chromium
CrCl ₃	: Chromium Chloride
Cu	: Copper
CVD	: Chemical vapour decomposition
C _o	: Initial concentration
C _e	: Final concentration
D-SIMS	: Dynamic – secondary ion mass spectrometry
EDX	: Energy dispersive X-ray
EELS	: Electron energy loss spectroscopy

H ⁺	: Hydrogen ions
HCl	: Hydrochloric acid
Hg	: Mercury
HNO ₃	: Nitric acid
IR	: Infrared
M-CNFs	: Modified carbon nanofibers
Mg g ⁻¹ / mg /g	: Miligram per gram
Mg L ⁻¹ /mg/L	: Miligram per litre
MWCNTs	: Multiwalled carbon nanotubes
N	: Nitrogen
NaOH	: Sodium Hydroxide
Ni	: Nickel
Nm	: nanometer
O	: Oxygen
Pb	: Lead
Pb(NO ₂) ₃	: Lead nitrate
Pd	: Palladium
pH	: Measure of acidic and basic of solution
ppm	: Part per million
R-CNFs	: Raw carbon nanofibers
rpm	: Revolution per minute
SAP	: Scanning atom probe
Se	: Selenium
SEM	: Scanning electron microscopy

Si	: Silicon
SIMS	: Secondary ion mass spectrometry
SPM	: Scanning probe microscopy
STEM	: Scanning transmission electron microscopy
STM	: Scanning tunnelling microscopy
S-SIMS	: Static – secondary ion mass spectrometry
TEM	: Transmission electron microscopy
TPD	: Temperature – programmed desorption
UPS	: Ultraviolet photoelectron spectroscopy
UV	: Ultra-violet
VACNF	: Vertically aligned carbon nanofiber
XPS	: X-ray photoelectron spectroscopy
Zn	: Zinc
°C	: Degree Celsius

CHAPTER 1

INTRODUCTION

1.1 Background of study

It is an undeniable fact the pollution of water resources due to the disposal of heavy metals has been causing worldwide concern. The major industries contributing to this problem are mining, metallurgical, chemical, tannery, battery manufacturing industries, fossil fuel, the modern chemical industry is bases largely on catalysts, many of which are metals or metal compounds, production of plastics, such as polyvinyl chloride, involves the use of metal compounds, particularly as heat stabilizers and etc. (Atieh, 2011).

The existence of excessive amount of heavy metals such as cadmium, chromium, copper, lead, mercury, nickel and zinc in an aqueous environment is a detriment because of their toxicity and carcinogenicity (Lu et al., 2006). Metals are non-degradable and can be accumulated in living tissues (Li et al., 2003).

For an example, lead poisoning in human will cause severe damage to the kidney, nervous system, reproductive system, liver and brain (Wang et al., 2007), while severe exposure of lead has been linked with sterility, stillbirths and neo-natal deaths (Wang et al., 2007).

Carbon is the main building block of a myriad of organic and inorganic matter around us. Carbon nanotubes (CNTs), a new-famous member of carbon family were first reported by Iijima in 1991(Li et al., 2003). The tubes consist of rolled up grapheme sheets, which exist as single-walled or multi-walled depending on their preparation conditions. CNTs have been experimentally proven to possess exceptional mechanical properties, unique electrical properties, high chemical and thermal stability and large surface area, attracting great attention in latent application (Li et al., 2003). Carbon nanofibers (CNFs) in the other hand, are produced using the same method as CNTs but at lower operating temperature. Both CNTs and CNFs

have shown capability of adsorbing heavy metals from the aqueous solution.

1.2 Problem statement

1.2.1 Problem identification

The contaminated effluents with heavy metals are undoubtedly a concern to the people. Many methods have been tried by the researchers in order to remove heavy metals which are precipitation, ion exchange, membrane filtration, electroplating, evaporation and adsorption. Among of these methods, adsorption is considered as the best method for heavy metals removal. A lot of adsorption methods have been developed and used to remove metal ions from wastewater such as granulated activated carbon, fly ash, peat, recycled alum sludge, peanut hulls, resins, kaolinite, manganese oxides, zeolite and biomaterials (Atieh, 2011).

In Malaysia, many freshwater resources such as river and lake are polluted by heavy metals. For examples, the Selangor river is contaminated with arsenic (As), mercury (Hg), cadmium (Cd), chromium (Cr), lead (Pb), zinc (Zn), copper (Cu), nickel (Ni), selenium (Se), and barium (Ba) (Fulazzaky et al., 2010). Besides, Tasik Chini is contaminated with lead (Pb), cadmium (Cd) and Copper (Cu) (Ebrahimpour and Mushrifah, 2007) while Juru River in Penang is contaminated with zinc lead (Pb), zinc (Zn) and copper (Cu) (Lim and Kiu, 1994).

In this study, carbon nanotubes (CNTs) and carbon nanofibers (CNFs) were used as the adsorbents in removing Pb(II) and Cr(III) from the aqueous solution by batch method. The influence of contact time and initial concentration of metals were investigated.

1.2.2 Significance of the project

By doing this study, the capability of CNTs and CNFs as the adsorbents to remove heavy metals which are lead nitrate $Pb(NO_2)_3$ and chromium chloride $CrCl_3$ were experimented. The efficiency of the absorbents in adsorbing those metals was examined.

1.3 Aim and objectives

1.3.1 Main aim

The aim of the research is to study the feasibility of carbon nanomaterials such as carbon nanotubes (CNTs) and carbon nanofibers (CNFs) in adsorbing heavy metals (lead and chromium).

1.3.2 Specific objectives

The objectives of the study are:

- To investigate the influence of the contact time on lead(II) and chromium(III) adsorption using CNTs and CNFs as the adsorbents.
- To study the effect of initial concentration on lead(II) and chromium(III) adsorption using CNTs and CNFs as the adsorbents.
- To examine the effect of initial pH on lead(II) and chromium(III) adsorption using CNTs and CNFs as the adsorbents
- To study the effect of temperature on lead(II) and chromium(III) adsorption using CNTs and CNFs as the adsorbents

1.3.3 Scope of study

- Investigation of the influence of the contact time in the adsorption process by varying the contact time by prolonging the contact time so that the equilibrium can be reached.
- Investigation of the effect of the initial concentration of heavy metals at different initial concentration. Different initial concentration of metal solutions can be achieved by dilution process.
- Study of the adsorption processes at different pH for both metal ions solution. Different pH can be achieved by adding sodium hydroxide or hydrochloric acid.

1.4 Relevancy of project

This project is important to be done; it investigated the capability of CNFs to be used as the adsorbents to adsorb heavy metals - lead (II) and chromium (III) which are hazardous to living organism.

1.5 Feasibility of the project

The project's scope covered the chemical engineering aspect where two types of parameters those influenced the adsorption process were studied. Doing this project, the understanding of adsorption process and its importance were enhanced.

Thus, this project – study of lead (II) and chromium (III) adsorption using carbon nanotubes (CNTs) and carbon nanofibers (CNFs) is feasible.

CHAPTER 2

LITERATURE REVIEW

2.1 Factors affecting the adsorption process

2.1.1 Effect of contact time

Increase of contact time will result to better adsorption capacity as reported by Atieh, (2011) and Chen and Wang, (2006).

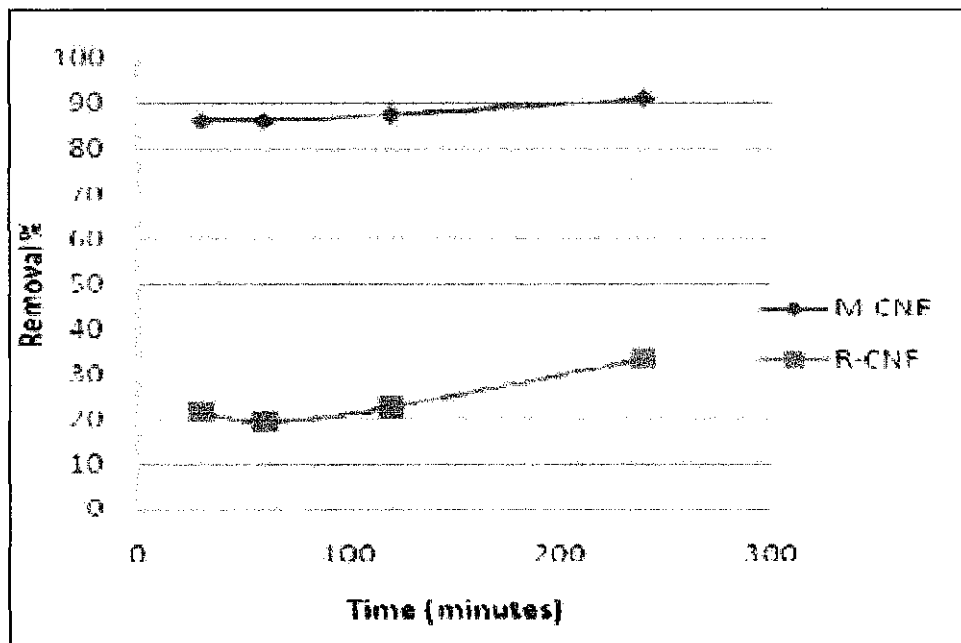


Figure 2-1: Effect of contact time on zinc removal using R-CNFs and M-CNFs at 150 rpm, pH 7 and 50mg (Atieh, 2011)

Figure 2-1 shows the percentage of removal at different contact time. It can be noted that as the contact time increased from 10 to 220 minutes, both of raw carbon nanofibers (R-CNFs) and modified carbon nanofibers (M-CNFs) had increased in removal. However, the increased of removal of R-CNFs is more significant than M-CNFs. It is believed that increase contact time will give more time for the adsorption process to take place and thus increasing the uptake.

2.1.2 Effect of initial metal concentration

High initial metal concentration will lead to better adsorption uptake as reported by Ahmed et al., (2010) and vice versa is reported by Atieh, (2011).

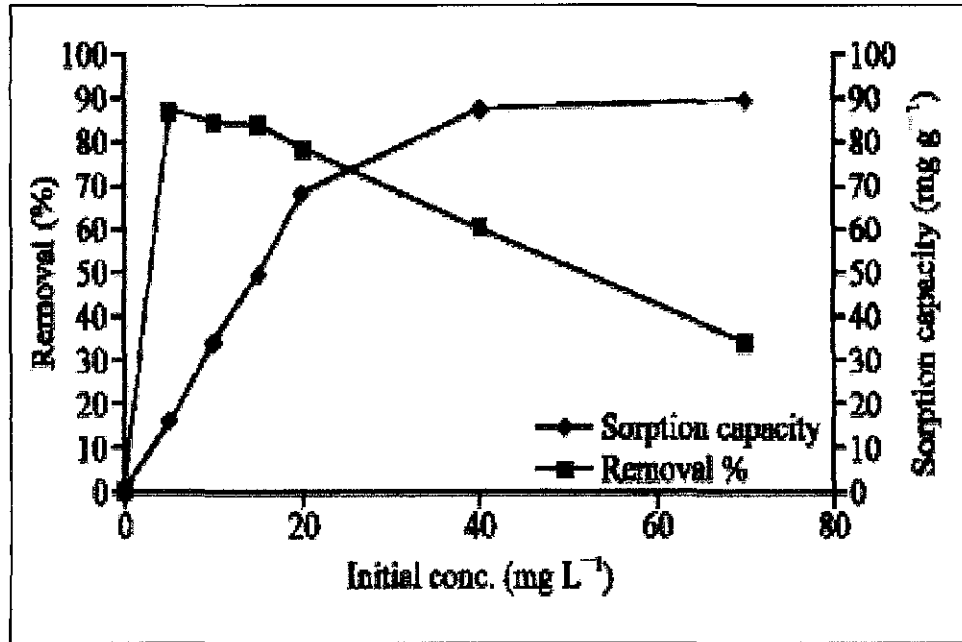


Figure 2-2: Effect of initial Pb concentration on sorption capacity and removal (Ahmed et al., 2010)

Figure 2-2 described that specific metal uptake increased with an increase in the sorbate concentration (Ahmed et al., 2010). The highest uptake of CNFs was around 89 mg g⁻¹ at the initial Pb concentration of 70 mg L⁻¹ with lowest sorption capacity of 15.77 (mg g⁻¹) at initial concentration of 5 mg L⁻¹ (Ahmed et al., 2010). The improvement in metal adsorption could be due to an increase in electrostatic interactions involving the site of progressively lower affinity for metal ions (Ahmed et al., 2010).

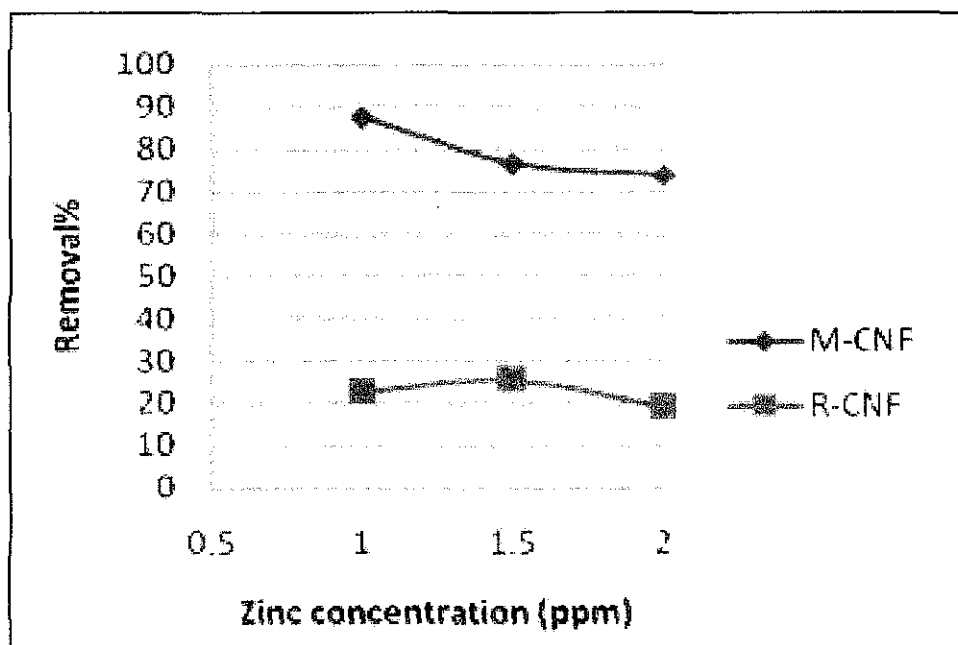


Figure 2-3: Effect of zinc concentration on percentage of removal of zinc at 150 rpm, pH 7 and 2 hr (Atieh, 2011)

In the experiment as reported by Atieh, (2011) various concentrations of zinc solution (1, 1.5 and 2) ppm were used in order to study their effect in percentage of removal as seen in Figure 2-3. It is clearly can be seen that the percentage removal of zinc decreases with increasing concentration using M-CNFs and there is no effect of R-CNFs on the removal of zinc at different concentration (Atieh, 2011).

2.1.3 Effect of pH

Higher pH value will lead to high metal removal as reported by Atieh, (2011), Ahmed et al., (2010), Wang et al. (2007), Stafiej and Pyrzyńska, (2007), Chen and Wang, (2006) and Li et al., (2003).

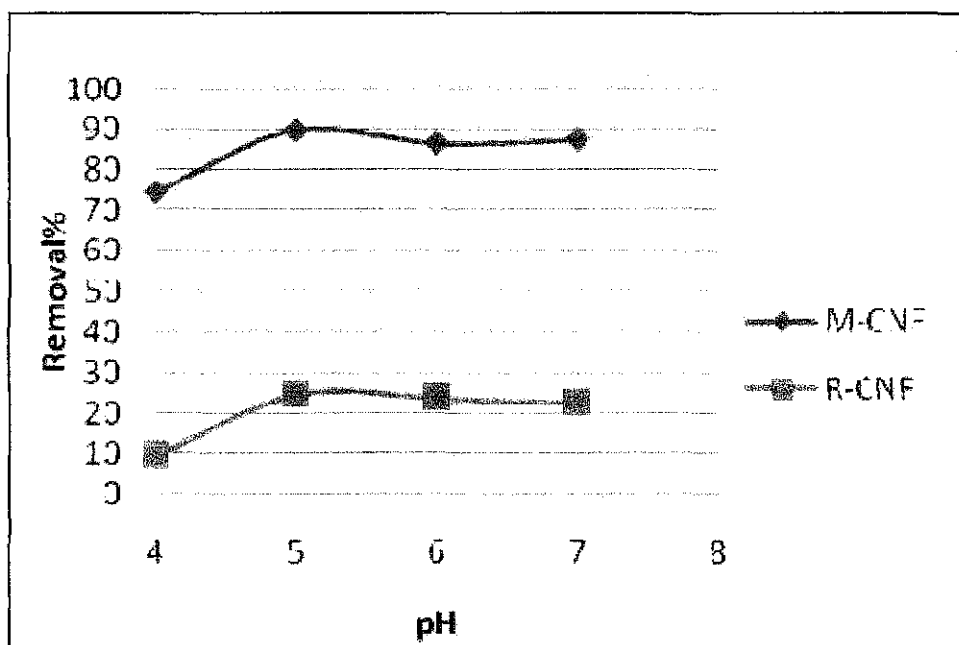


Figure 2-4: Effect of modified CNFs (M-CNFs) and raw CNFs (R-CNFs) on the removal of zinc at different pH (Atieh, 2011)

One of the main parameters that control the adsorption of ion solid-water interfaces is pH of the aqueous solutions (Atieh, 2011). Figure 2-4 shows the effect of pH on the adsorption of zinc used as a model of divalent metal ion on R-CNFs and M-CNFs. Maximum removal of zinc species was achieved at pH 5, it can be observed that, around 20% removal of zinc was obtained by R-CNFs and 90% of removal of zinc was achieved by M-CNFs. The M-CNFs which was functionalized with carboxylic (COOH) functional group increase the adsorption rate of CNFs due to strong interaction between the ions positive charges and functional groups negative charges (Atieh, 2011).

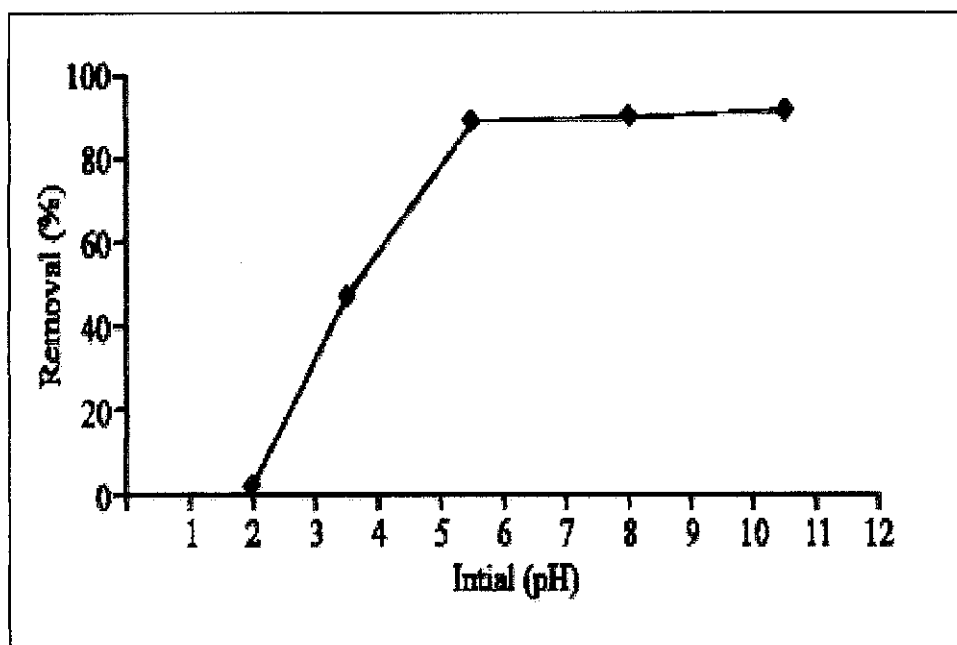


Figure 2-5: Effect of pH on removal of Pb using CNFs (Ahmed et al., 2010)

Figure 2-5 shows the effect of pH. The lead removal recorded its minimum pH value at pH 2 which can be justified on the basis that at lower pH values, the H^+ ions compete with the metal cation for the adsorption sites in the system (Ahmed et al., 2010). Maximum removal was obtained at pH 5.5 and it remained constant at higher pH where the removal occurs due to precipitation at pH higher than 6.

2.1.4 Effect of temperature

Increase in temperature will lead to better adsorption uptake as reported by Chen and Wang, (2006) and Lu et al., (2006). According to Lu et al., (2006), the increase in metal uptake is due to the release of H^+ ions from the surface sites of adsorbent (CNTs), where the metal ions (Zn^{2+}) are then adsorbed onto the surface sites and thus lead to a decrease in solutions' pH.

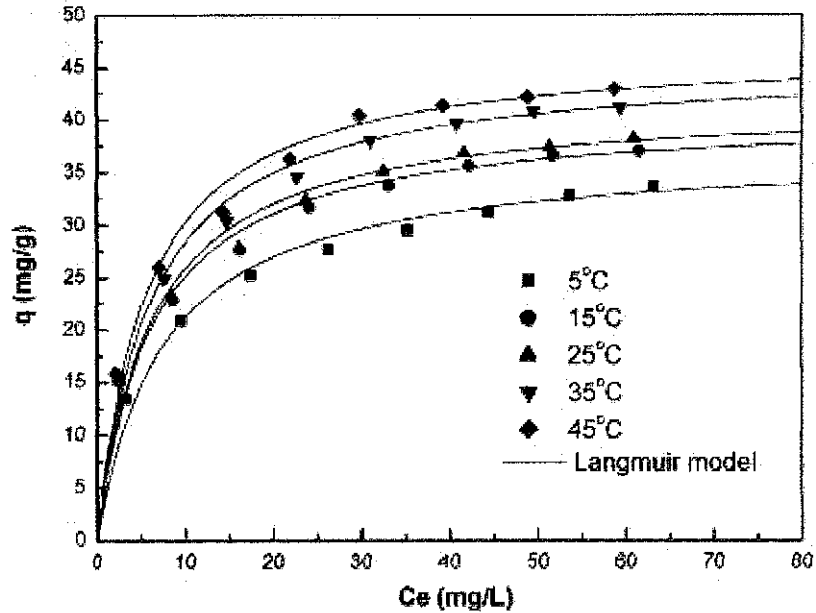


Figure 2-6: Langmuir isotherm of Zn(II) sorption by multiwalled carbon nanotubes (MWCNTs) at various temperatures (Lu et al., 2006)

Figure 2-6 shows the plot of Langmuir isotherm of Zn(II) by MWCNTs. It can be seen that the adsorption capacity of MWCNTs increase with a rise in temperature and high capacity was observed at 35 and 45°C.

2.1.5 Effect of adsorbent dosage

The effect of adsorbent dosage was studied by Atieh, (2011), Sharma and Gad, (2010) and Li et al., (2003). Two different findings were reported. Sharma and Gad, (2010) and Li et al., (2003) are in agreement that increased in adsorbent dosage will increase the adsorption capacity.

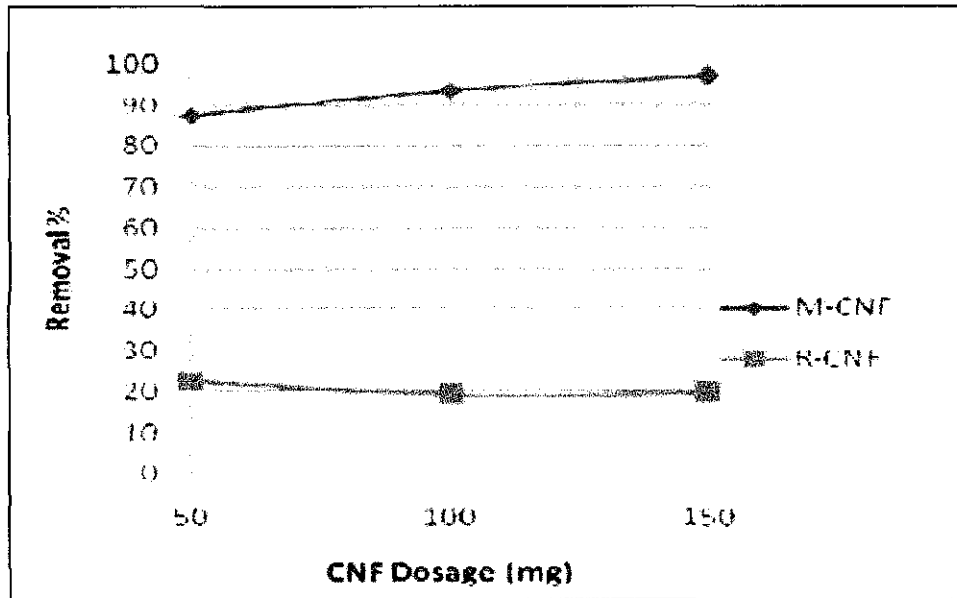


Figure 2-7: Effect of CNFs' dosage on percentage of removal of zinc at 150 rpm, pH 7 and 2 hr (Atieh, 2011)

However, from Atieh, (2011), the influence of zinc sorption on CNFs dose was studied by varying the CNFs dosage from 50mg to 150 mg. as seen in Figure 2-7. From the figure, it can be observed that 97% of zinc was removed using M-CNFs at 150mg dosage. It suggests that after solution reaches its saturated phase, the maximum adsorption sets in and hence the amount of ions bound to the adsorbent and the amount of free ions remain constant even further addition of dose of adsorbent (Atieh, 2011).

2.1.6 Effect of agitation speed

The influence of the agitation speed was studied by Atieh, (2011). Figure 2-8 shows the effect of agitation speed by varying the speed from 100 rpm to 200 rpm. The removal of efficiency of M-CNFs increases as the agitation speed increases, giving us an idea that increases in agitation speed improves the diffusion of zinc ions towards the CNFs' surface (Atieh, 2011). However, a fluctuation of percentage of removal can be seen when R-CNFs is used.

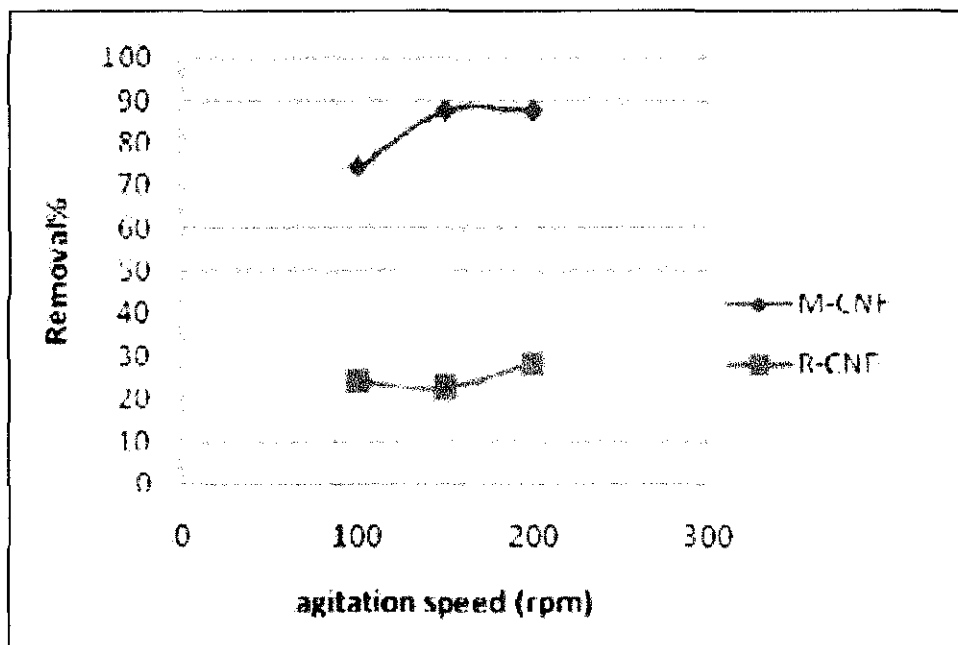


Figure 2-8: Effect of agitation speed on percentage removal of zinc at pH 7 and 2 hr (Atieh, 2011)

2.1.7 Effect of functionalization

In the latest research concerning the topic (Atieh, 2011), discussed the effect of functionalized CNFs in removing Zn(II) ions from water. It is found that the carboxylic functionalized CNFs are better than raw CNFs in adsorption process.

(Wang et al., 2007) studied the removal of Pb(II) from aqueous solution by adsorption onto manganese oxide-coated carbon nanotubes. From the research, it is observed that MnO₂/CNTs adsorbent is better than pristine CNTs.

Adsorption of Ni(II) from aqueous solution using oxidized MWCNTs/HNO₃ (Chen and Wang, 2006) was studied. From the research, it is discovered that oxidized MWNTs has better uptake capacity in comparison with pristine MWCNTs, thus in agreement with (Wang et al., 2007). Besides, it is realised that the uptake capacity is optimum at pH 8.

2.2 Functionalization of carbon nanofibers (CNFs)

Functionalization can be described as the addition of functional group onto the surface of a material. In CNFs context, the functionalization process can be defined as the addition of functional groups onto the CNFs surfaces.

2.2.1 Carbon Nanofibers and Carbon Nanotubes functionalization

Figure 2-9 shows the schematic representation of a CNF. Unlike CNTs which structure is cylindrical, CNFs structure is consisting of multitude of small graphite layer separated with each other and it increases the likelihood of functionalization. While for CNTs, the possible functionalization types can be seen in Figure 2-10. For CNTs, there are two possible ways of doing functionalization which can be either endohedral (inside CNTs) or exohedral (outside CNTs). In CNTs case, covalent functionalization of functional groups only can be done at the nanotube end or defects (Guzeliya, 2008).

CNFs is undoubtedly advantageous of its large surface area for active reaction sites (Lee and Im., 2010) and thus functionalization process or modification is done in order to acquire some properties of the CNFs for examples to have better electrical, dispersion, physical and metal removal properties.

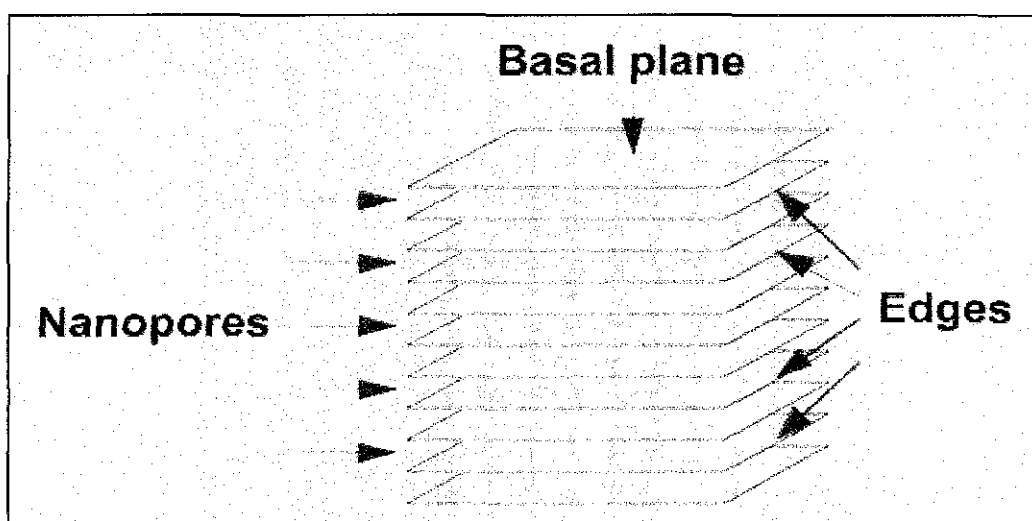


Figure 2-9: Schematic representation of a carbon nanofiber consisting of a multitude of small graphite layers separated at a distance of 0.35 nm (Rodriguez, 2000)

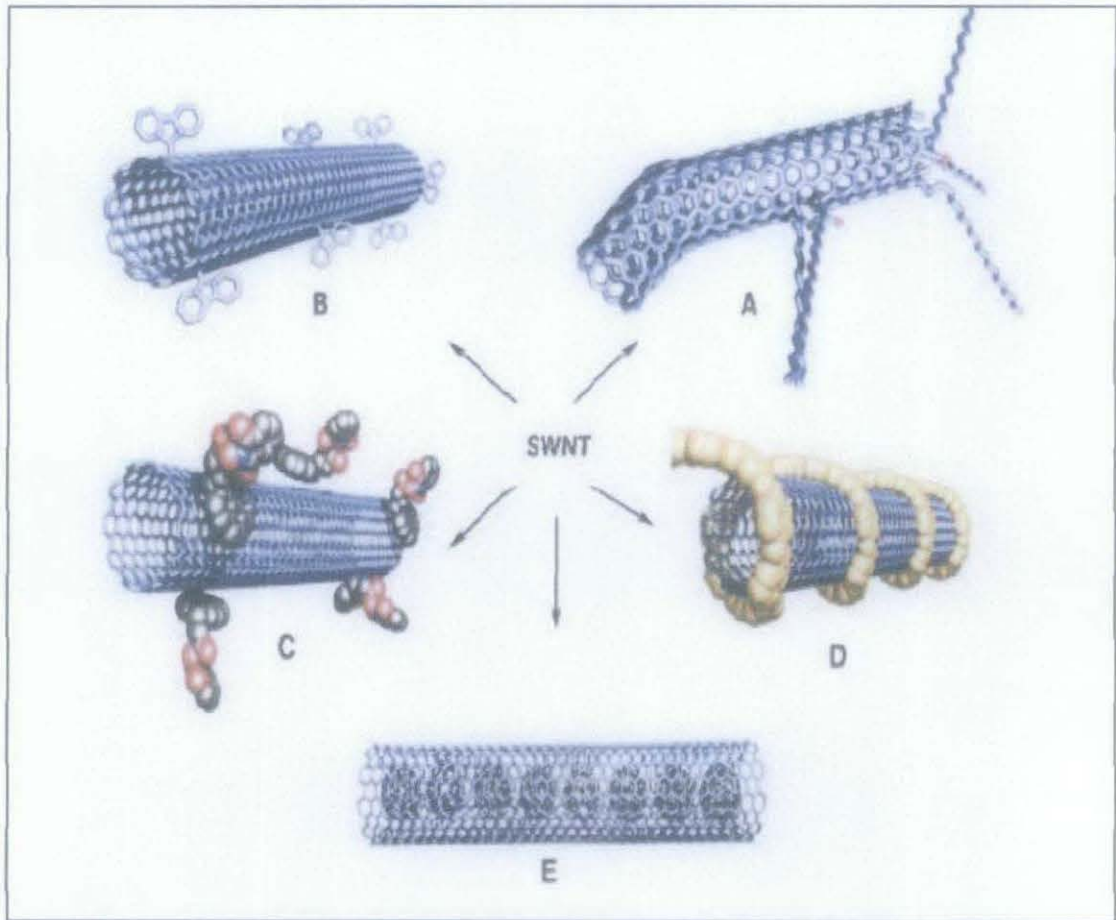


Figure 2-10: A) defect-group functionalization, B) covalent sidewall functionalization, C) noncovalent functionalization with surfactants D) noncovalent functionalization with polymers and E) endohedral functionalization (Korneva, 2008)

It is known that surface properties are often differ from the bulk material properties due to differences in physical structure and chemistry (Klein et al., 2008). Besides, the surface is a dynamic system that interacts with environment, giving the idea that the characteristic can be exploited for many applications. Nanostructured materials' surfaces are special because of their enhanced role in determining functional properties which more pronounced as the surface-to-volume ratio increases (Klein et al., 2008).

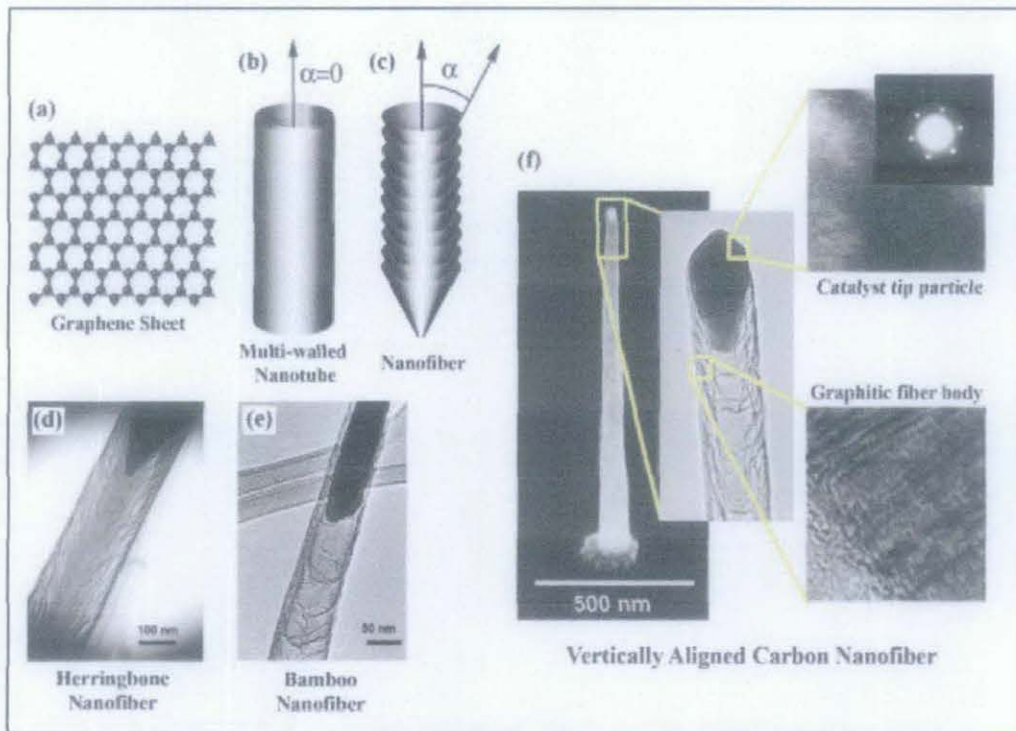


Figure 2-11: Schematic of carbon nanostructures a) single sheet of graphite, b) CNT consisting of concentric grapheme sheets, c) CNF composed of stacked grapheme cones at an angle α with respect to the axis of the fiber. The two primary CNFs structures: d) herringbone-type CNF and e) bamboo-type CNF f) vertically aligned CNF composed of a Ni catalyst nanoparticle at the tip and a graphitic fiber body (Klein et al., 2008)

Figure 2-11 shows (a) a CNT, more specifically a single-walled CNT, which can be considered as a graphene sheet, rolled into a cylinder where multiple concentric sheets create a MWCNT as can be seen in (b), by introducing five and seven member rings into the grapheme will allow the formation of curved structures such as “buckyballs” and nanocones. However, CNFs are a class of these materials that have curved grapheme layers or nanocones stacked to form a quasi-one-dimensional filament, whose internal structure can be characterized by the angle α between the grapheme layers and the fiber axis as seen in (c). One general distinction observed is the difference between the two main CNFs types: “herringbone” (d), with dense conical grapheme layers and large α , and “bamboo” (e), with cylindrical cuplike grapheme layer and small α , which is more similar to MWCNT but in the case of a true CNT, the value of α is zero (Klein et al., 2008). Regardless of distinct differences in the internal structures, CNFs are often called CNTs as they can display

similar morphology to MWCNTs but the physical and chemical properties are different. Nanotubes are reported to display ballistic electron transport and diamond like tensile strength along the axis, nanofibers have proven the robustness as individual, freestanding structures with higher chemical reactivity and electron transport across their sidewalls, important for functionalization and electrochemical application (Klein et al., 2008).

2.2.2 Surface characterization techniques

This section will discuss the experimental surface characterization work by technique with brief explanation of each technique.

Scanning probe microscopy (SPM)

SPM technique surveys small area of surface with high lateral resolution. SPM techniques include scanning tunnelling microscopy (STM) and atomic force microscopy (AFM) (Klein et al., 2008).

- Scanning tunnelling microscopy (STM)

STM maps the surface of electrically conductive material with sub-Angstrom vertical resolution. STM observations are used by Parades et al to address the atomic scale reorganization of the CNF surface after oxidation (Klein et al, 2008).

- Atomic force microscopy (AFM)

The obvious advantage of AFM is that it can generate high lateral resolution images with superb z-height discrimination from all types of surfaces, even those that are wet or insulating. Besides, AFM is sensitive to chemical changes via molecular recognition and friction imaging, otherwise known as chemical force microscopy. An AFM-based approach was developed to resolve hydrophilic oxygen group regions on carbon surfaces which work on the detection of phase changes in the noncontact tapping mode of AFM. Parades et al. (2002) applied this approach to detect and map the oxygen functionalized content of CNFs surfaces. However, phase image contrast is a relative measure within a given

image limiting sample to sample comparisons (Klein et al., 2008).

Infrared (IR) spectroscopy

IR spectroscopy is a robust and easy method for characterization of surfaces with the addition of the interferometer. Surface sensitive IR techniques can probe depths of a few centimetres to as shallow as 100nm below the surface. Meanwhile CNFs are generally on the order of 20-200nm in diameter, the spectra convey “bulk” chemical information. However, this can be useful to distinguish which surface groups are present (Klein et al., 2008). An example, Ros et al., (2002) compared the surface structure of untreated bamboo-type to herringbone-type CNFs using transmission IR. Herringbone fibers, in which the sidewalls terminate with greater number of reactive graphitic edges was hypothesize, would be more susceptible to surface oxidation than bamboo CNFs. By putting the transmission levels from each sample the same, the fibers are compared in Figure 2-12. Overall, Ros et al., (2002) concluded that the CNFs have a defect-rich structure and the carbon-hydrogen bonds are present on herring as well as bamboo fibers (stretching at 3012, 2947, 2917 and 2846 cm^{-1}). However, noted that only herringbone fibers showed evidence of carbonyl groups (1717-1712 stretch) and a loss of mass as CO_2 when annealed.

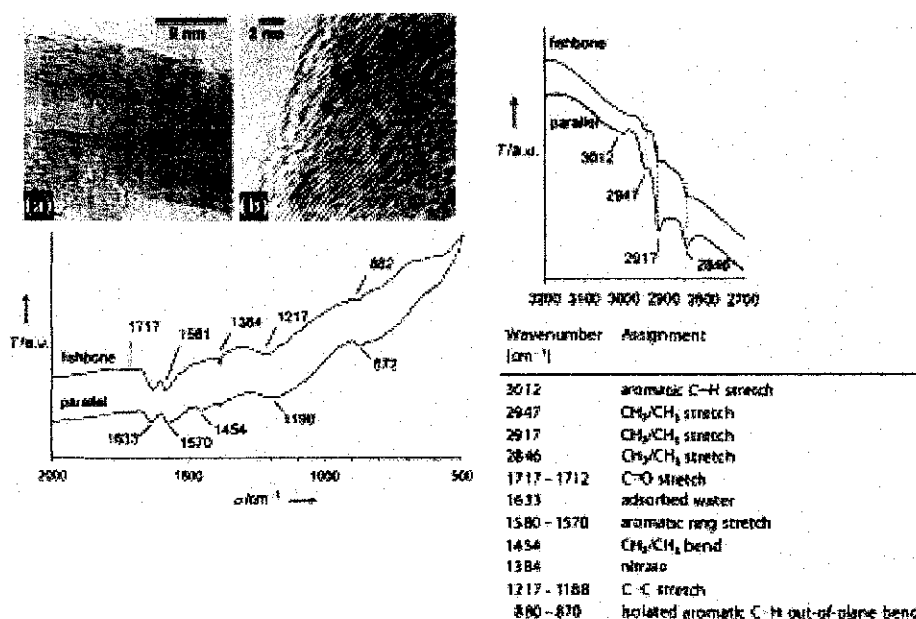


Figure 2-12: TEM of untreated (a) fishbone (herringbone) and (b) parallel (bamboo) CNFs with the corresponding IR spectroscopy results (Ros et al., 2002)

Electron spectroscopy

When x-rays of sufficient frequency (energy) interact with an atom, inner shell electrons in the atom will get excited and move to the outer, emptying the orbitals or they may be ejected from the atom completely and thus ionizing the atom (Klein et al., 2008). Some of the techniques are:

- X-ray photoelectron spectroscopy (XPS)

XPS works using an x-ray source with energy in the keV range, the escape depth of core-level photoelectron is only several atom layers deep with a lateral spatial resolution from $\sim 30\mu\text{m}$ to a few millimeters. The data produced permit the detection of all elements except hydrogen and helium with a sensitivity of higher than 1 at % (Klein et al., 2008).

- Ultraviolet photoelectron spectroscopy (UPS)

UPS is almost the same with XPS but it uses ultraviolet radiation (10-50 eV) to excite valence-level photoelectron of much lower kinetic energies (Klein et al., 2008).

- Auger electron spectroscopy (AES)

A general advantage of AES is that the yield of Auger electrons is highest for the lighter elements such as C, Si, N and O. Besides, the incident electron beam can be focused to a fine spot giving excellent lateral spatial resolution on the order of a few tens of nanometers (Klein et al., 2008).

Electron microscopy

Scanning electron microscopy (SEM) is perhaps the most widely and frequently used method of characterizing the morphological structure and topography of a sample. Transmission electron microscopy (TEM) and scanning transmission electron microscopy (STEM) are not only conveying information about the nanostructure as a whole, but also show the presence of surface interface by high-resolution TEM (HRTEM). An energy dispersive X-ray (EDX) is a common companion tool to both SEM and TEM which readily gives the elemental composition of the sample and useful in generating elemental maps (Klein et al., 2008).

- Scanning electron microscopy (SEM)

SEM is the most widely used surface imaging technique; the depth from which the relevant secondary electrons typically escape (usually ranging from 5-10 nm deep depending on the material) results in the image containing both surface and bulk information. Brightness and image contrast can also be ambiguous and not quantitatively topographical where edges are often highlighted and surface charging can result in large fluctuations in signal level as well as in distortions of the scan raster (Klein et al., 2008).

For an example, Xia et al., (2005) shows morphological change in the fiber surface as seen in Figure 2-13. The morphological transition from a smooth fiber (a) to one with protrusions from the surface in (b), agrees with the processing steps used to grow secondary fibers from iron oxide particles deposited on the oxidized CNFs.

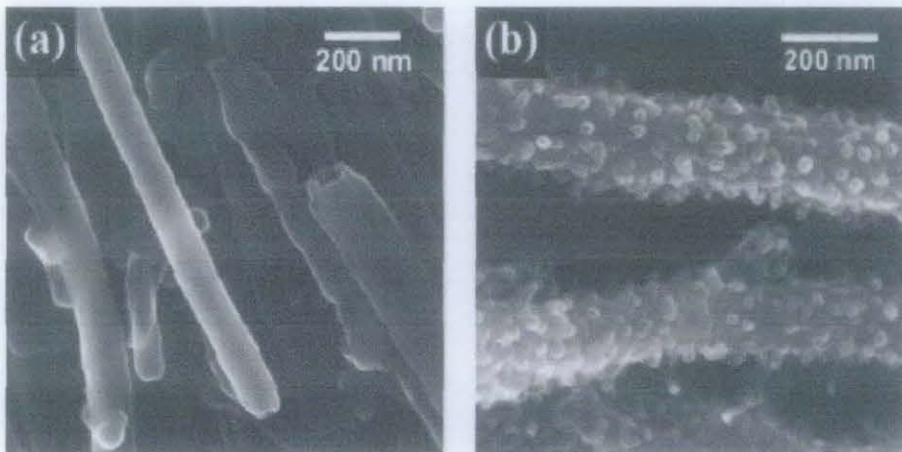


Figure 2-13: SEM images of plasma treated CNFs (a) before and (b) after a 5 min growth of secondary nanofibers (Xia et al., 2005)

- Transmission electron microscopy (TEM)

STEM and TEM can be used to analyze the surface as well as internal structure of CNFs. Both real space (“image”) and reciprocal space (“diffraction”) data together with chemical and electronic analytical information (derived from EDX or EELs), can be obtained from the same nanoscale area. Therefore, TEM and

STEM can provide a wide deep range of data about the specimen of interest (Klein et al., 2008).

For an instance, a study of nanofiber structural effects of different catalysts (Ni versus Pd) was done by Ominami et al., (2005). It can be observed in Figure 2-14 that the Ni-catalyzed fibers have graphitic planes ending on sidewalls of the fiber in a herringbone fashion, whereas the Pd-catalyzed fibers have multiwalled nanotube-like layers on the outer walls of the fiber. Ominami et al., (2005) credited the increased electrical conductivity along the length of the Pd-catalyzed CNFs to the improvement in the graphitic structure and lower interface resistance with the substrate.

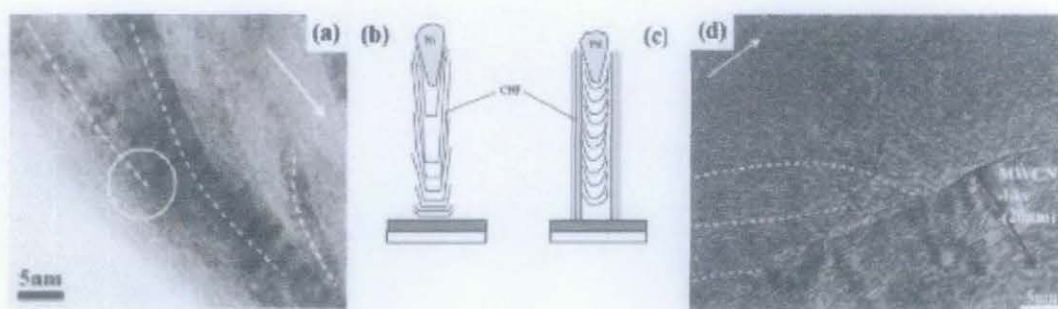


Figure 2-14: STEM images and cartoons of the nanofiber outer wall structure [(a) and (b)] using a Ni catalyst and [(c) and (d)] using Pd catalyst. The white arrows in the STEM images points towards the catalyst particles at tip of the fiber (Ominami et al., 2005)

- Electron energy loss spectroscopy (EELS)

EELS used to measure the energy spectrum of the electron beam transmitted through the sample in the TEM or STEM which contains chemical data, which are complementary to those derived from EDX, but with much higher sensitivity for the lower atomic number elements ($Z < 20$) (Klein et al., 2008).

Secondary ion mass spectrometry (SIMS)

SIMS is a powerful characterization tool with outstanding surface sensitivity on the scale of a few atomic layers. SIMS provides detection limits surpassing those attainable with XPS (Klein et al., 2008). There are two types of SIMS experiments, dynamic SIMS (D-SIMS) and static SIMS (S-SIMS).

- **Dynamic SIMS (D-SIMS)**

D-SIMS used a continuous, high-flux stream of primary ions having an energy of 1-20 keV bombards the surface and fragments it as much as possible to maximize the generation of charged atomic species which serves a second purpose of eroding (sputtering) the sample's surface for elemental depth profile information (Klein et al., 2008).

- **Static SIMS (S-SIMS)**

Opposite of D-SIMS, the aim of S-SIMS is to maintain the molecular integrity of the surface fragments as much as possible. Thus, a pulsed source is often used, the primary beam flux is reduced, and the beam is rastered to generate larger charged sample fragments. Due to the fact that many detected species are not distinctly identifiable, S-SIMS is only qualitative (Klein et al., 2008).

Temperature-programmed desorption (TPD)

TPD is often called as thermal desorption spectroscopy (TDS), is a method of characterizing adsorbed surface species by heating the sample under vacuum and simultaneously detecting the residual gas by means of a mass spectrometer. As the temperature rises, certain adsorbed species will have enough energy to escape or desorb from the surface and will be detected as a rise in pressure for a particular component (Klein et al., 2008).

Atom probe

Atom probe is an instrument used to combine a probe-aperture field ion microscope (with atomically high resolution) and a mass spectrometer (with single particle sensitivity). The scanning atom probe (SAP) work by field evaporating surface atoms from the sample for mass analysis. Therefore, for field improvement purposes, protruding, high aspect ratio structures are suggested (Klein et al., 2008).

2.2.3 Surface modification techniques

It is very vital to control the surface chemistry of CNFs in order to define their functionality. Either it used for microfluidic or intracellular devices, the surface charge, hydrophobicity or chemical reactivity of CNFs can be altered through both physical and chemical modifications.

Chemical vapour deposition of thin film coatings

Deposition of a thin film coating on the external surface of a CNF provides a means to impart special properties and functionality nanofibers which may be far beyond the scope of those attainable with the carbon nanostructure alone, thereby making coatings an extremely useful component (Klein et al., 2008). Due to high aspect ratio limited line-of-site access to the CNF bases, the most common approaches to thin film coatings for nanofibers are chemical vapour depositions (CVDs) routes. Some of the examples are:

- In situ PECVD (Plasma-enhanced CVD) coatings and surface modification

PECVD involved in the catalytic synthesis of carbon nanostructures where the aim is not only to control the internal graphitic structure but also significantly affect the condition of the nanofiber structure. Figure shows how the cone angle can be controlled by changing the source/etchant gas ratio.

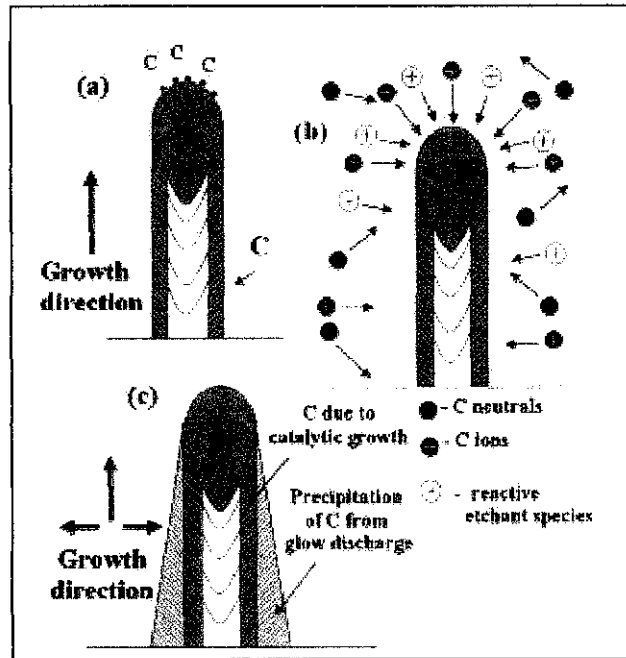


Figure 2-15: Schematic representation of the growth of (a) a CNF using conventional thermal CVD, (b) vertically aligned carbon nanostructure using PECVD, and (c) a carbon nanocone formed due to additional precipitation of C on the outer walls during PECVD (Klein et al., 2008)

- CVD of oxides and nitrides

Basically, the most common coatings deposited on both CNFs and CNTs via CVD methods is silicon oxide and the process of coating hollow CNFs with nitride are with aims to acquire some properties for the CNFs (Eg; to acquire hydrophilic properties) (Klein et al., 2008).

- CVD of polymers

Besides, several groups have also coated CNTs and CNF with polymer thin films using CVD routes (Klein et al., 2008).

- Atomic layer deposition (ALD)

ALD occurs similarly to standard CVD with an exception that in an ALD process the CVD reaction is broken into two half-reactions, keeping the precursor materials separate throughout of the process (Klein et al., 2008).

Electro- or electroless plating

The introduction of electrically addressable vertically aligned carbon nanofiber-VACNF material has enabled a multitude of electrochemical modification strategies (Klein et al., 2008).

Extremely high surface area metallic electrodes have been demonstrated by Metz et al, 2006 using electroless deposition of gold onto herringbone-type VACNFs as shown in Figure 2-16. Exposed graphite planes of the vertical carbon material were first functionalized with carboxylic acid site using photochemical capture and deprotect of the methyl ester of undecylinic acid under nitrogen-purged 254nm irradiation (Klein et al., 2008).

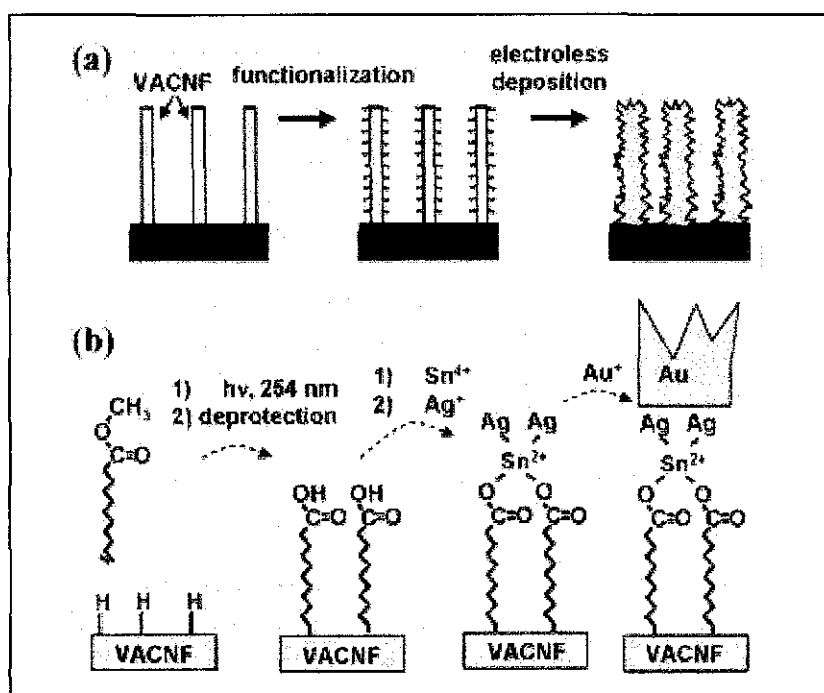


Figure 2-16: (a) Schematic illustration of the steps involved in the functionalization of CNFs and subsequent procedure for electroless deposition. (b) chemical transformations involved in the nanofiber modification (Klein et al., 2008)

Chemical functionalization

Graphitic materials, when they are in their original state and free of surface oxygen group are hydrophobic in nature. However, following routine activation procedures, these materials can exhibit some degree of hydrophilic character. The chemical stability of CNFs allows their surface chemistry to be controlled with variable wettability both hydrophobic and hydrophilic. Chemical, biochemical and electrochemical functionalization of VACNF material are usually preceded by an oxidation step in which amorphous material is removed and oxygen-containing moieties are generated on the surface. The most commonly noted are carboxyl surface terminus species (Klein et al., 2008). Some examples of chemical functionalization are:

- **Wet etch treatment**

Wet etch treatment is based on recalcitrance of low defect-harboring CNT material, early attempts with carbon nanostructure functionalization employed aggressive acidic pretreatment methods (Klein et al., 2008). For an example, Ros et al., (2002) surveyed several surface oxidation methods and concluded that a mixture of concentrated nitric and sulfuric acids was the most effective methods for attaching oxygen containing surface groups to defect sites on the nanofiber surface (Klein et al., 2008).

- **Plasma treatment**

Surface treatment of mesocarbonmicrobeads found that oxygen plasma oxidized the carbon surface, resulting in the formation of acidic groups, where in contrast, nitrogen and ammonia plasma treatments produced basic functionalities (Klein et al., 2008).

- **Photochemical functionalization**

Photochemical functionalization is a technique that allows the UV-induced reaction of $-H$ groups on the nanofiber sidewalls with alkenes terminated molecules (Klein et al., 2008).

- Thermal treatment

Thermal treatment in oxidizing atmospheres has been reported to removal of amorphous material and for the oxidation of graphitic material to chemically create functionalized group (Klein et al., 2008).

- Addition of linkers and polymers

Addition of linkers and polymers is done by adding covalent addition of linker molecules and polymer to improve CNFs functionality.

2.3 Review remarks

From literature research that has been done, it was discovered that both CNFs and MWCNTs have the capability as the adsorbents to adsorb Cu (II), and Pb(II) from the aqueous solution. The modified CNFs and MWCNTs are better than pristine CNFs and MWCNTs as the adsorbents. pH, contact time, temperature, adsorbent dosage, metal concentrations and modifications done to CNFs or MWCNTs are among of the factors influencing the adsorption uptake.

CHAPTER 3

METHODOLOGY

3.1 Preliminary research analysis

For preliminary research analysis, related journals and papers concerning the topic were searched. They were reviewed, the results those were important were noted and recorded.

3.2 Laboratory work

In this research, CNTs and CNFs were used as the adsorbents to remove lead(II) and chromium(III) in the aqueous solution, 4 parameters were varied which were:

- Contact time
- Initial concentration
- pH
- Temperature

Chemicals and adsorbent used

Table 3-1: List of chemicals and adsorbent used

Chemicals	Purity (%)
Lead nitrate $Pb(NO_2)_3$	99
Chromium Chloride $CrCl_3$	99
Hydrochloric acid, HCl	95-98
Sodium Hydroxide (NaOH)	99
Multiwalled carbon nanotubes (CNTs)	95
Carbon nanofibers (CNFs)	99.4 (self-synthesized)

Experimental set up

Table 3-2: Equipment/tools required for experiment

Equipment used	Purpose
Test tube (25 ml) + stopper	To fill in chemical samples
Volumetric flask (250ml& 100ml)	For metal solution preparation
Graduated cylinder (50ml)	To measure volume of metal solution
Pipet	For metal solution preparation
Funnel	For metal solution preparation
Test tube rack	To place sample test tube
Beaker	For miscellaneous purpose
Digital weigh	For adsorbents (CNTs and CNFs) weight measurement
Stopwatch	To record agitation time between samples and adsorbents
Glass plate/ Petri dish	To be used for adsorbents measurement
Atomic absorption spectrometer (AAS)	To test concentration of heavy metals remained
Bath shaker	To provide shaking motion to samples and adsorbents
Ultra-Filtrator	To filtrate the (CNTs and CNFs) after the adsorption process
Surface area analyser	To test surface area of adsorbent (CNTs and CNFs)
pH analyser	To measure the pH

3.3 Experimental methods

3.3.1 Experimental flow

Figure 3-1 shows the experimental flow of the adsorption process.

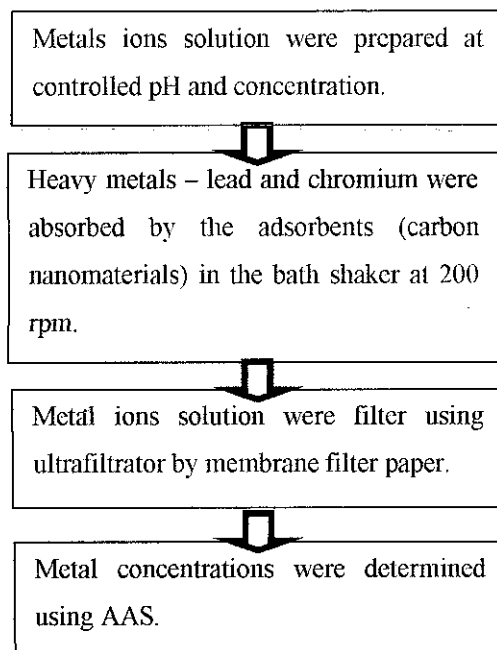


Figure 3-1: Adsorption process experimental flow

3.3.2 BET surface area and pore size distribution testing

Using surface area and pore size analyser, the BET surface area and pore size distribution of CNFs and CNTs were tested. It was determined by the adsorption of N_2 gas at 77K onto the sample. It determines surface area measuring the amount of nitrogen gas adsorbed as a function of pressure. Figure 3-2 shows the surface area and pore size analyzer.



Figure 3-2: Surface area and pore size analyzer

3.3.3 Batch adsorption studies

The metal adsorption experiments were carried out at room temperature (25°C). The metal solution were placed in a conical flask and agitated using a rotary shaker at constant speed. After the experiments, the metal concentrations were tested using atomic absorption spectrometer (AAS) as seen in Figure 3-3.



Figure 3-3: Atomic adsorption spectrophotometer (AAS)

3.3.4 Metal solution preparation

Depending on the variable, for an example pH, the metal solutions were prepared according by diluting the metals powder in respective amount of deionised water using 1000ml volumetric flask. The pH of solution was controlled by addition of 0.1M NaOH and 0.1 M HCl.

For lead (Pb), five different solutions concentration are prepared, they were, 3, 6, 9, 12, 15 ppm, while for chromium, (Cr), 5, 10, 15, 20, 25 ppm solutions concentration were prepared.

3.3.5 Effect of contact time of metal adsorption

The same methods were repeated as in Section 3.3.1. In order to investigate the effect of the contact time of metal adsorption, the samples were taken at different contact time. For lead, the contact time were 1,2 ,3 and 4 hours, while for chromium, the contact time were, 0.33, 0.67, 1,2,4,6, and 24 hours.

3.3.1 Effect of initial metal concentration on metal uptake

For initial metal concentration, preliminary analysis were done at lower metal ions concentrations which were 3,6, 9, 12, 15 ppm for lead and using both of CNFs and CNTs. The scheduled experiments were done using CNFs adsorbent for both metals – lead and chromium. The initial metals concentrations were increased from 5, 10, 15, 20 to 25 ppm for both lead and chromium. The other parameters were kept constant throughout of the experiment. Figure 3-4 shows the bath shaker used in the adsorption process.



Figure 3-4: Bath shaker used in the adsorption process

The solutions were filtered using membrane filter paper using ultrafiltrator. The concentrations of the remaining metal ion in the solution, C_e were measured by Atomic Adsorption Spectrophotometer (AAS).

$$\% \text{ Adsorption} = (C_o - C_e)/C_o \times 100$$

C_o and C_e are the initial and final concentration of the adsorbate respectively.

3.3.2 Effect of pH

In order to study the effect of pH, 8 different pH were used ranging from pH 1 – 12. They were pH 1, 3, 5, 6, 7, 9, 11 and 12. The others parameters were kept constant throughout of the experiment.

3.3.3 Effect of temperature

In order to investigate the influence of temperature, 3 different bath temperatures were used; they were 25, 35 and 45°C. The temperatures were varied by using the temperature controlled bath shaker. The remaining parameters were kept constant throughout of the investigation.

3.3.4 Adsorption isotherms model

Two types of isotherms – Langmuir and Freundlich were developed from the experimental data in describing the adsorbate concentration and the degree accumulation onto the adsorbents. The Langmuir isotherm assumes that the adsorption is a single layer adsorption process. The linearized Langmuir isotherm can be written as Eq. 1:

$$C_e/Q_e = 1/x_m K + (1/x_m)C_e \quad (1)$$

where C_e is final concentration of solution after adsorption (mg/L), x_m is the monolayer sorption capacity, K is the constant related to adsorption energy and Q_e is the amount of metal adsorbed per unit mass of adsorbent (mg/g).

Freundlich isotherm assumes that the adsorption of adsorbate onto the adsorbent's surface is a multilayer adsorption process. The model can be represented in the following linearized form Eq 2:

$$\log Q_e = \log K_f + (1/n) \log C_e \quad (2)$$

where K_f is the multilayer sorption capacity, C_e is the final concentration of solution after adsorption (mg/L), $1/n$ is the Freundlich intensity parameter and Q_e is the amount metal adsorbed per unit mass of adsorbent (mg/g).

3.3.5 Metal concentration determination using AAS

Metal concentrations before and after the adsorption process were determined using AAS. AAS – atomic absorption spectrophotometer is equipment which designed to determine the amount (concentration) of an object element in a sample, utilizing the phenomenon that the atoms in the ground state absorb the light characteristic wavelength passing through an atomic vapour layer of the element (B. General Test , 2001).

3.4 Gantt Chart for the First Semester of FYP

Figure 3-5: Gantt chart for the first semester of final year project

No	Project Activities	Week no.														
		1	2	3	4	5	6	7		8	9	10	11	12	13	14
1	Approval of selected project topic	■	■													
2	Preliminary research work		■	■	■	■										
3	Submission of extended proposal defence						■									
4	Proposal defence									■	■					
5	Project work continues • Metal adsorption experiment commenced											■	■	■		
6	Submission of interim draft report														■	
7	Submission of interim report															■


■ : Process


■ : Completed milestone

3.5 Gantt Chart for the Second Semester of FYP

Figure 3-6: Gantt chart for the second semester of final year project

No	Project Activities	Week no.															
		1	2	3	4	5	6	7		8	9	10	11	12	13	14	15
1	Project work continues <ul style="list-style-type: none"> • Experiment continued • Result analysis 																
2	Submission of progress report																
3	Project work continues																
4	Pre-EDX																
5	Submission of draft report																
6	Submission of dissertation (soft bound)																
7	Submission of technical paper																
8	Oral presentation																
9	Submission of project dissertation (hard bound)																

 : Process

 : Completed milestone

CHAPTER 4

RESULTS AND DISCUSSION

4.1 BET Surface area carbon nanomaterials

Carbon nanofibers (CNFs) and carbon nanotube (CNTs) surface areas were analysed using surface area analyser. The BET surface areas of CNFs were found to be 194.99 m²/g, while for CNTs, the BET surface area was found to be 478.99 m²/g.

4.2 Pore size distributions

In this section the pore size distributions of CNFs and CNTs will be discussed.

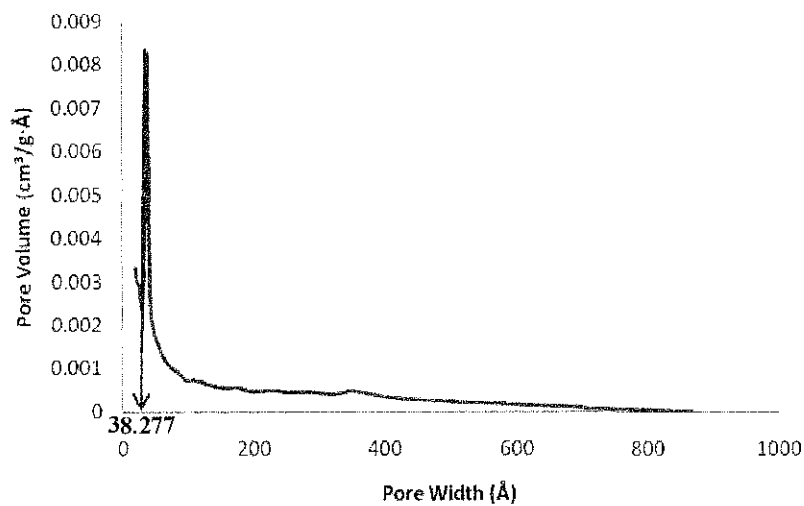


Figure 4-1: Pore size distribution of carbon nanofibers (CNFs)

Figure 4-1 shows pore volume, (cm³/g·Å) versus the pore width, (Å) of carbon nanofibers. From the results, the pore volume is highly dominated by pore width of 38.2767 Å which cover pore volume of 0.00831 cm³/g·Å. It shows that CNFs is a mesoporosity adsorbent of 38.2767 Å which is equal to 3.82767 nm. It is in between 2 - 50 nm and thus it is classified as mesopores. The distribution of the pore can be classified as in Table 4-1.

Table 4-1: Classification of pore size (IUPAC)

Type of pore	Typical size
Macropore	>50 nm
Mesopore	2-50 nm
Micropore	0.8-2 nm
Sub-micropore	<0.8nm

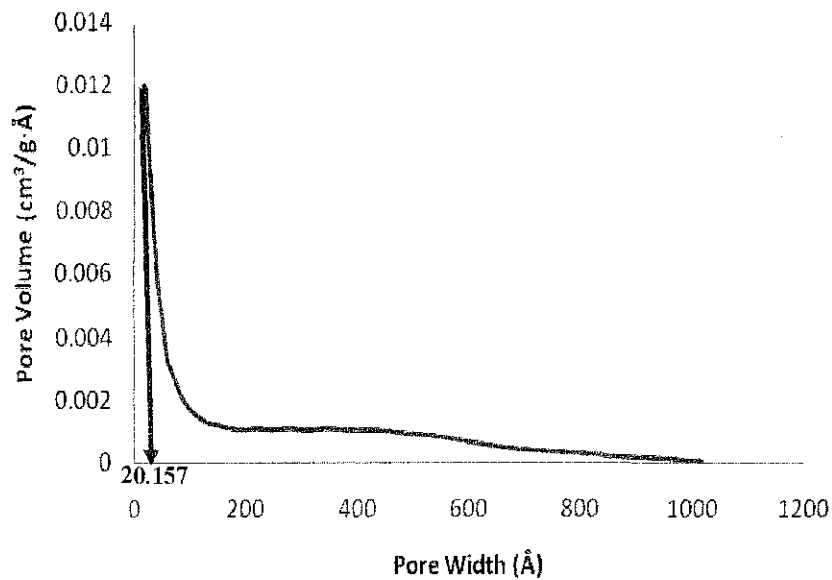


Figure 4-2: Pore size distribution of carbon nanotubes (CNTs)

Figure 4-2 shows the pore size distribution of CNTs. The pore volume is highly dominated by pore width of 20.1572 Å which involves pore volume of 0.012032 cm³/g·Å. Thus, it can be seen that CNFs is mesoporsity adsorbent with pore width of 20.1572 Å or 2.01572 nm.

4.3 Adsorption isotherm of adsorbents using liquid nitrogen

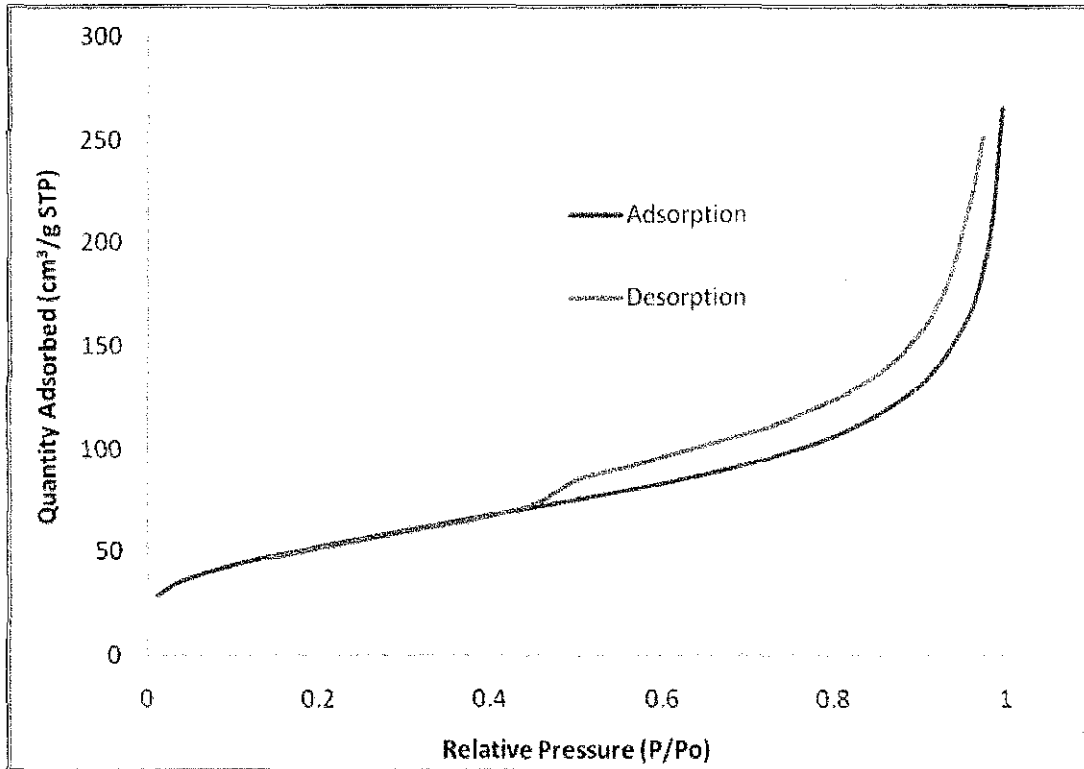


Figure 4-3: Adsorption isotherm of carbon nanofibers (CNFs)

Figure 4-3 shows the graph of the quantity adsorbed cm^3/g versus relative pressure, p/p° of liquid nitrogen adsorption by CNFs. The adsorption behaviour is parallel with to Type IV adsorption isotherm where it tends to level off and later exhibit hysteresis loop. The maximum adsorption is at relative pressure of $0.974038499 \approx 1$ where the quantity adsorbed is $266.0562 \text{ cm}^3/\text{g}$. While, the desorption process starts at relative pressure of 0.974038499 with the amount of decrement of 251.6537 .

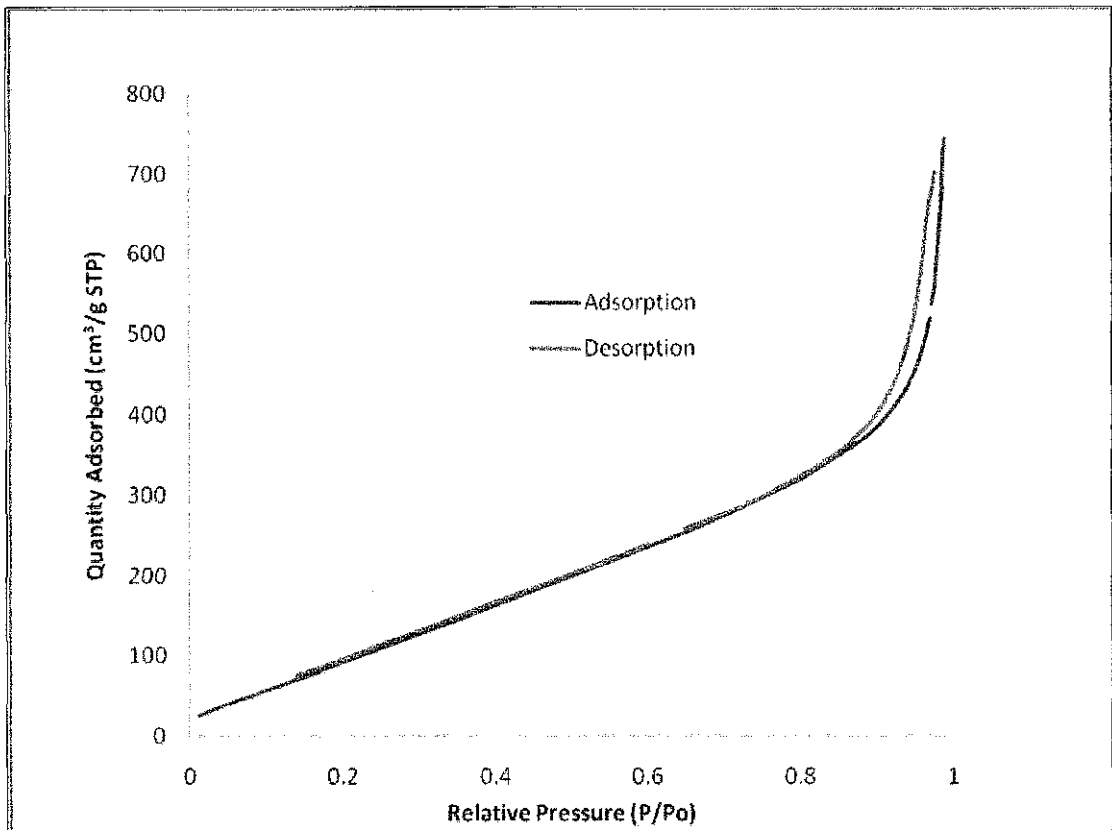


Figure 4-4: Adsorption isotherm for carbon nanotube (CNTs)

Figure 4-4 describes the graph of the quantity adsorbed cm^3/g versus relative pressure, p/p° of liquid nitrogen adsorption by CNTs. The adsorption behaviour is parallel with to Type IV adsorption isotherm where it tends to level off and later exhibit hysteresis loop. The maximum adsorption is at relative pressure of 0.98934 ≈ 1 where the quantity adsorbed is $742.9766 \text{ cm}^3/\text{g}$, while, the desorption process starts at relative pressure of 0.97679 and the amount of decrease to 702. 6079.

4.4 Pre-experimental analysis

The purpose of the pre-experimental analysis is to have a direct comparison between CNFs and CNTs as the adsorbents. The comparison was done at low initial metal concentrations using lead ion solutions.

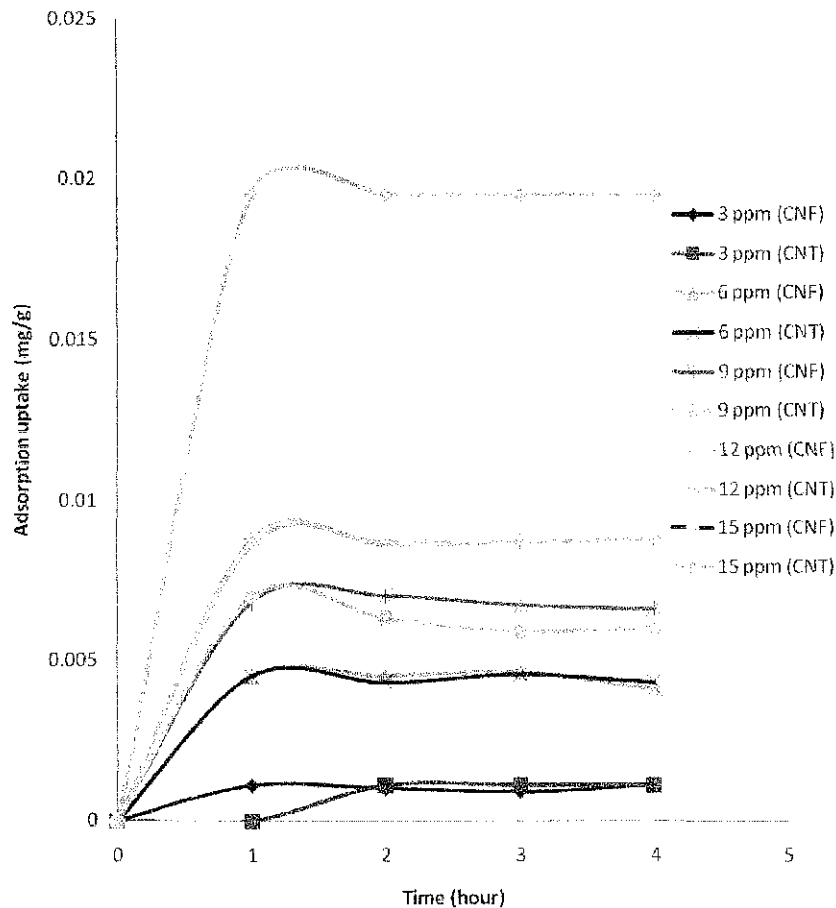


Figure 4-5: Comparison between CNFs and CNTs adsorbents on lead adsorption at different initial concentrations

Figure 4-5 shows the comparison of CNFs and CNTs as the adsorbents on lead adsorption process at different initial concentrations. It is observed that, using CNFs are almost as effective as CNTs in adsorbing the lead. At 9 ppm initial metal concentration, CNFs shows better adsorption characteristic after 4 hours in comparison with CNTs. However, at the other concentrations, the adsorption uptakes are almost the same. Hence, it can be seen that CNFs is as good as CNTs at low initial metal concentrations. Therefore, the experiments were proceeded with CNFs

as the adsorbent due to good potential of CNFs as better adsorbent than CNTs. CNFs is said to be better than CNTs due to its structure. CNFs consists of multitude of small graphite layer separated with each other and it increases the possibility of fluid diffusion in comparison with CNTs which consists of long cylindrical nanotubes.

4.5 Effect of contact time on metals adsorption

Figure 4-6 and Figure 4-7 are referred in order to study the effect of contact time. As the contact time increases, the adsorption increases and they become stable. Based on Figure 4-7, chromium adsorption reaches plateau at 6 hours.

For lead adsorption, as shown in Figure 4-6, it can be noted that the uptake is much lower at 24 hours in comparison with 6 hours, suggesting that the adsorption process has not reached equilibrium at 6 hours where the adsorption process is much higher than desorption process in comparison with the adsorption and the desorption rate at 24 hours. For all the experimented adsorption processes, it can be noted that the adsorption increases as the contact time increases. Thus, it is in agreement with Atieh (2011) and Chen and Wang (2006).

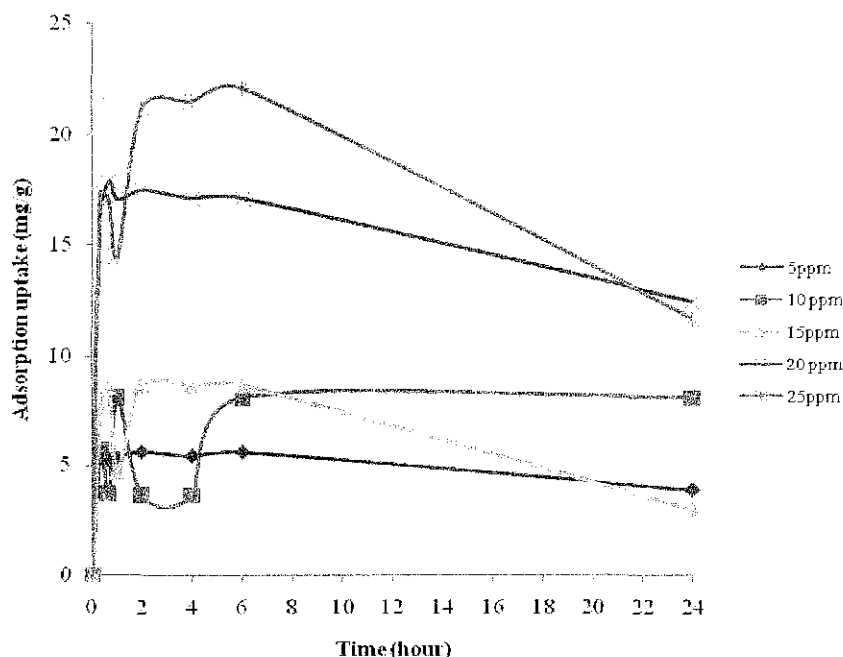


Figure 4-6: Effect of contact time on lead adsorption at different initial metal concentrations using CNFs, at pH 6, adsorbent dosage of 1g/litre, 25°C and 200 rpm

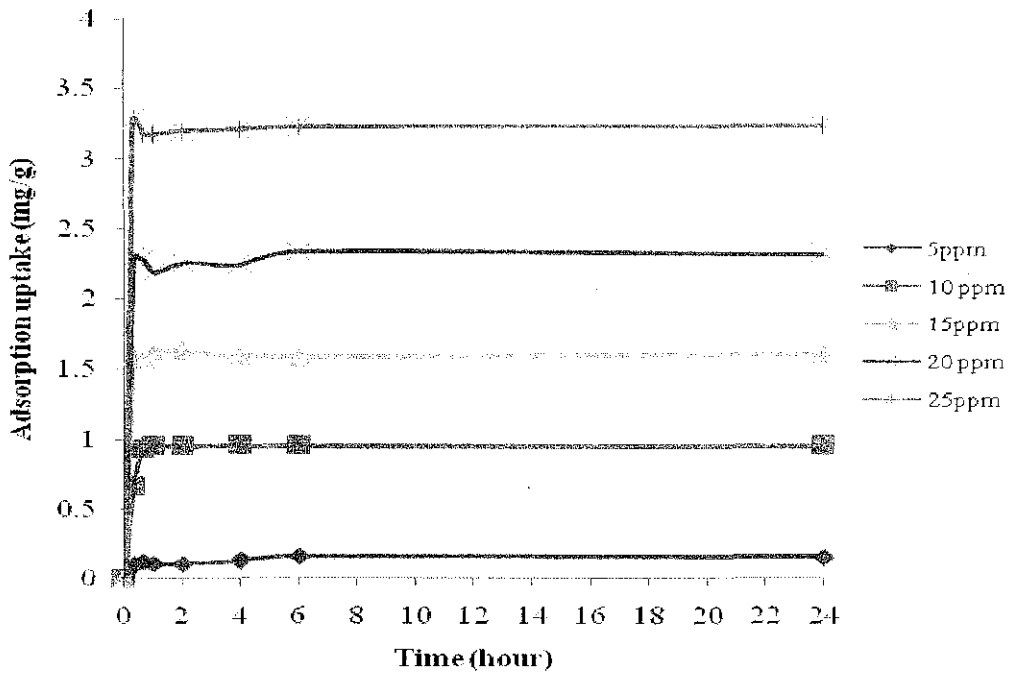


Figure 4-7: Effect of contact time on chromium adsorption at different initial metal concentrations using CNFs, at pH 6, adsorbent dosage of 1g/litre, 25°C and 200 rpm

4.6 Effect of initial concentration on metals adsorption

In order to study the effect of initial concentration of lead adsorption, Figure 4-8 and Figure 4-9 are referred. In both of the experiments, five different initial concentrations were used. From the observations made, the higher lead initial concentration, the higher the adsorption uptake showing that at higher initial concentration of lead, the adsorbents (CNFs and CNTs) able to absorb the metals. The finding is in agreement as reported by Yehya et al.

Figure 4-6 shows the effect of initial concentration for lead. It can be seen that as the initial concentration of lead increases, the adsorption uptake increases until it reached an optimum limit which is 20 ppm. When the initial concentration of lead is increased, the adsorbate/adsorbent ratio is higher at constant dosage of adsorbent. Suggesting that there are limited adsorption site available at higher lead concentration, thus, the adsorption process is limited (Yehya et al., 2010).

The effect of initial concentration for chromium is shown in Figure 4-7. It can be noted that, increase of initial concentration of chromium will lead to better adsorption uptake. In this case, the optimum limit has not reached. Hence, the CNFs are capable of adsorbing the metals without yet exceeding the limitation of the optimum uptake at constant CNFs dosage – 1g/litre.

This is because, the adsorbents used (CNFs and CNTs) are nanoparticles. Thus, using a little amount of adsorbent (in the experiment it is 1mg/L of adsorbent) is enough in order to adsorb the metals. It is because smaller particles will give higher surface area. Hence, higher initial concentration of leaf will result to high adsorption uptake at the same amount of adsorbent used.

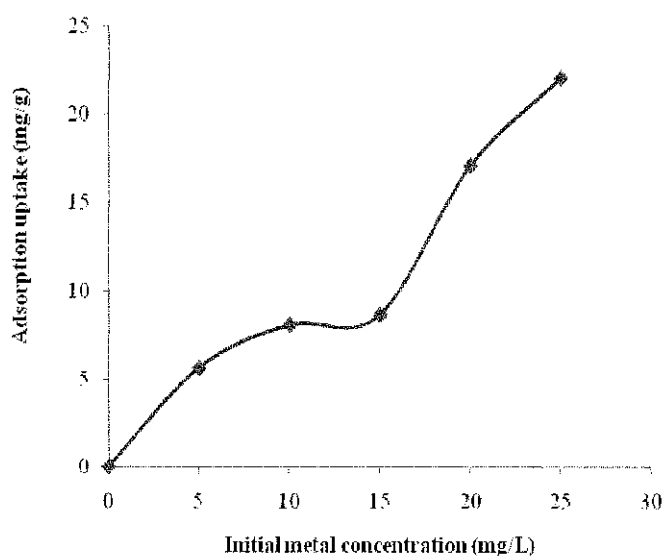


Figure 4-8: Effect of initial metal concentration on lead adsorption using CNFs, adsorbent dosage of 1g/litre, 25°C, pH 6 and 200 rpm

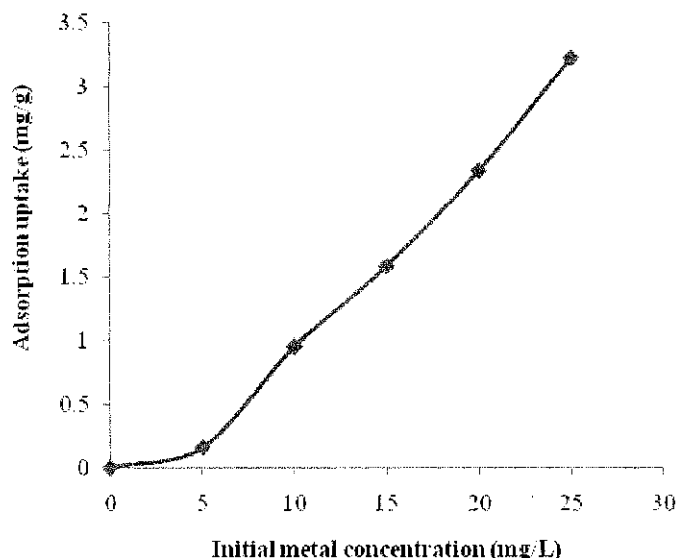


Figure 4-9: Effect of initial metal concentration on chromium adsorption using CNFs, adsorbent dosage of 1g/litre, 25°C, pH 6 and 200 rpm

4.7 Effect of pH on metals adsorption

The pH's influence on the adsorption uptake can be seen in Figure 4-10 and Figure 4-11. For chromium, as described in Figure 4-11, the metal uptake is low at pH 1-3 and it is nearly constant and optimum at pH ranging from pH 5 to pH 9 and start to decrease at pH 10. According to Agrawal et al., (2008), at pH ≈ 1 , H_2CrO_4 (neutral form) is the predominant species of Cr(VI) hence less metal ions attraction to CNF surface.

At higher pH, there will be OH^- in aqueous solution, causing hindrance between negatively charged ions, CrO_4^{2-} (chromate), $Cr_2O_7^{2-}$ (dichromate) and negatively charged adsorbent, which decrease the adsorption (Gupta et al., 2010).

For lead, as seen in Figure 4-10, difference in pH of metal solution leads to fluctuating data of lead uptake. The lowest and highest lead uptake is 0.8891 mg/g and 22.095 mg/g at pH 12.36 and 9, respectively.

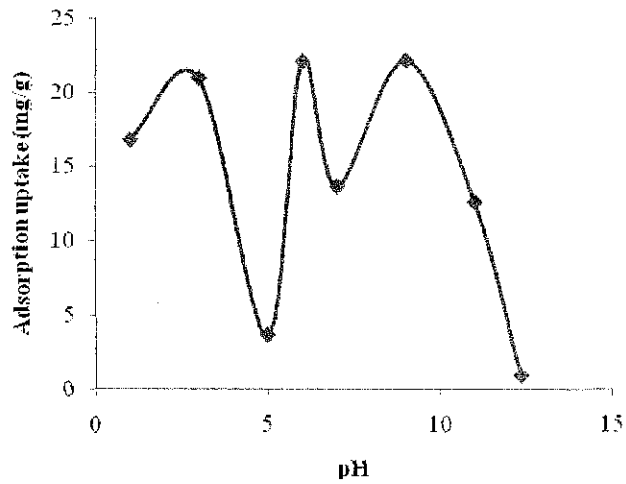


Figure 4-10: Effect of solution's pH on lead adsorption using CNFs, at 25 ppm lead concentration, adsorbent dosage of 1g/litre, 25°C and 200 rpm

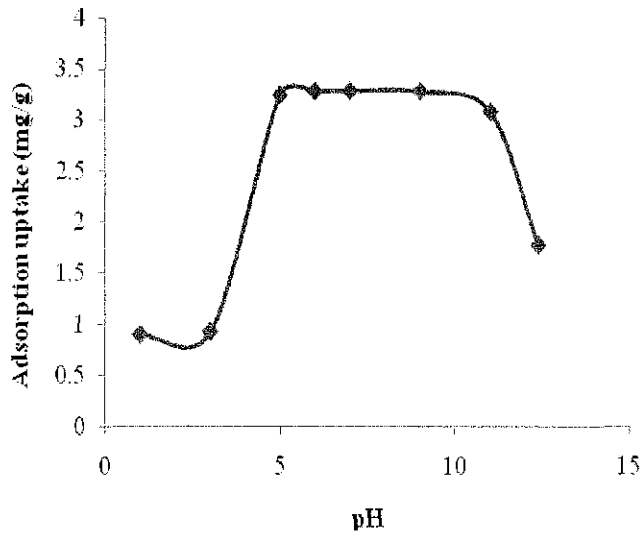


Figure 4-11: Effect of solution's pH on chromium adsorption using CNFs, at 25 ppm chromium concentration, adsorbent dosage of 1g/litre, 25°C and 200 rpm

4.8 Effect of temperatures on metals uptake

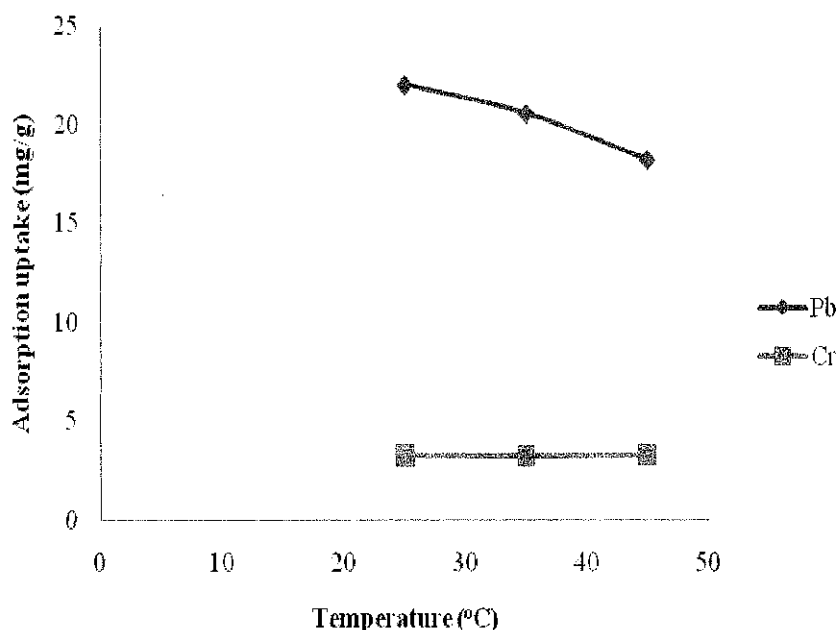


Figure 4-12: Effect of temperature on lead and chromium adsorption using CNFs, at pH 6, adsorbent dosage of 1g/litre, 25 ppm and 200 rpm

The influence of the temperature on the adsorption process can be seen in Figure 4-12 for both lead and chromium adsorption. Both of the metals show different behaviour of adsorption uptake as the temperature increases from 25°C to 45°C. For lead, it is clearly can be seen in Figure 4-12 that the adsorption uptake decreases as the temperature increases. This can be explained from the fact that high temperature will promote desorption thus decreasing the uptake.

For chromium, it is found that the adsorption is independent of temperature. Increase in temperature does not give any significant changes on the metal uptake.

The difference in adsorption can be described by the affinity of metal adsorption. Reported by Sharma and Gad, (2010), affinity of adsorption of chromium is better than lead using hebba clay and activated carbon as the adsorbents.

The behaviour of lead and chromium metals ions can be described from ionic radius perspective, reported by Srivasta et al., (2007), smaller ionic size of ion is easier to be adsorbed in comparison with bigger ionic size ion. In this study, lead ion's size is

much bigger than the chromium ion's size, the ionic radii of lead and chromium are 1.19Å and 0.52Å respectively. For chromium, since the ionic size is much smaller, at higher temperature, the desorption and adsorption can occur simultaneously. Thus, the metal uptake is independent of temperature. However, for lead, the ionic size is much bigger, high temperature will excite the metal ions in the adsorption site thus promoting desorption of the ions. The adsorption site is then emptied, and competition between hydrogen ions and lead ions in occupying the adsorption site will occur. Since lead ions are bigger in size, the surface adsorption is much difficult. Thus, as the temperature increases, desorption of lead ions are promoted.

4.9 Adsorption isotherm of metals adsorption process

Two types of isotherms – Langmuir and Freundlich were developed from the experimental data. Langmuir isotherm is based on single layer adsorption. While the Freundlich isotherm is based on multilayer adsorption process.

4.9.1 Langmuir isotherm

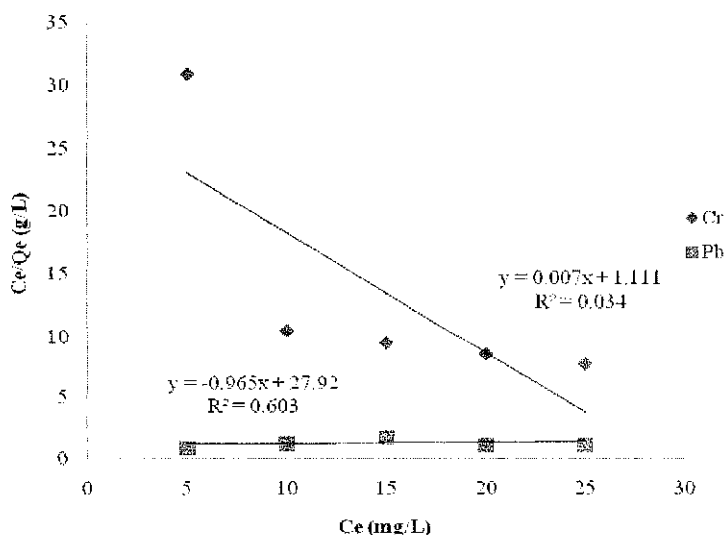


Figure 4-13: Langmuir isotherm for chromium adsorption

Figure 4-13 shows the Langmuir isotherm for lead and chromium adsorption. The R squared value of adsorption process is 0.034 and 0.603 respectively.

4.9.2 Freundlich Isotherm

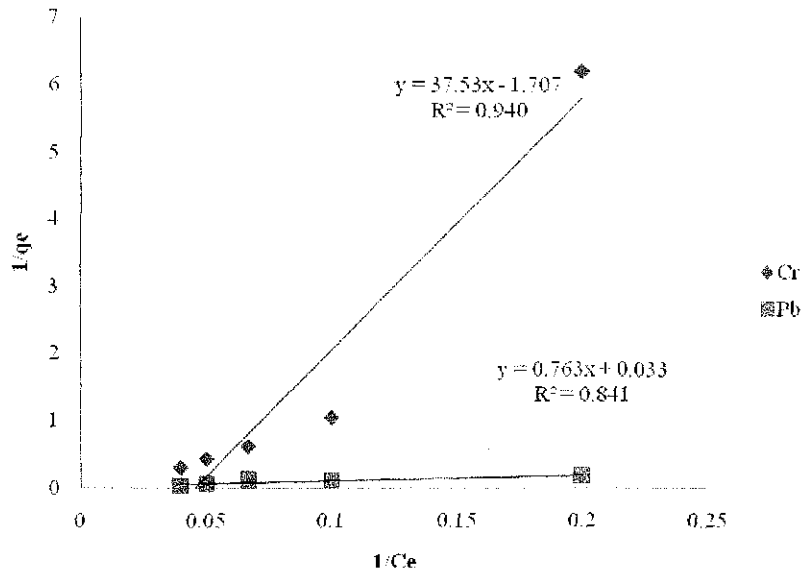


Figure 4-14: Freundlich isotherm for chromium adsorption

Figure 4-14 displays the graph $\log Q_e$ versus $\log C_e$ with respect to Freundlich isotherm. Comparing the R-squared value for both of the models, it can be observed that both of the adsorption processes fitted Freundlich isotherm better than Langmuir isotherm. The R-squared value is 0.8541 for lead adsorption and 0.9702 for chromium adsorption showing that the adsorption processes are multilayer.

CHAPTER 5

CONCLUSION AND RECOMMENDATION

5.1 Conclusion

Carbon nanofibers (CNFs) and carbon nanotubes (CNTs) have a great potential as the adsorbents to remove metal ions in the adsorption process. CNFs is observed to be as effective as CNTs in adsorbing lead ions. Increase in contact time will increase the adsorption uptake. Chromium adsorption achieved equilibrium at 6 hours of reaction for all metal concentrations while the highest lead uptake is 22.095 mg/g at 6 hours contact time with 25 ppm concentration. For efficient adsorption, high metal concentrations are favourable in wastewater treatment process. CNFs is efficient to be used as adsorbent for chromium adsorption as it is optimum at neutral pH and lead uptake is highest at pH 9. Temperature does not give much influence to chromium and lead adsorption. However, for lead, the adsorption uptake decreases as temperature increases. The adsorption processes fitted Freundlich isotherm better than Langmuir isotherm indicating that the adsorption processes are multilayer.

5.2 Recommendations

5.2.1 Functionalization of carbon nanomaterials

Carbon materials are hydrophobic, thus it is very difficult for them to dissolve in water. Thus, by functionalizing, functionalized group can be attached to the carbon nanomaterials, improving the dissolving criteria and the metals attraction characteristics.

5.2.2 Analysis on adsorbent used

The adsorbents – CNFs and CNFs those had been used for adsorption processes can be analysed. By doing the analysis, surface's structure changes can be detected and compared with the adsorbents before the adsorption process.

5.2.3 Calibration of Atomic Absorption Spectrophotometer (AAS)

Calibration of AAS is important in order to prevent interference. Interference can be described as any factor that affects the ground state population of the analysed element and any factor that may affect the ability of the instrument to read the parameter. By doing calibration, interferences can be detected and eliminated (Ma and Gonzalez, 2011).

REFERENCES

- Ahmed Y.M., Al-Mamun A. Muyibi S.A., Al-Khatib M.F.R., Jameel A.T and AlSaadi M.A. (2010). Study of Pb adsorption by carbon nanofibers grown on powdered activated carbon, *Journal of Applied Sciences* 10(17): 1983-1986, 2010 ISSN 1812-5654.
- Agrawal A., Pal C., and Sahu K. K. (2008). Extractive removal of chromium (VI) from industrial waste solution, *Journal of Hazardous Materials*, 159 (2008) 458-464
- Atieh, M.A, (2011). Effect of functionalized carbon nanofibers with carboxylic function group on the removal of zinc from water, *International Journal of Environmental Science and Development*, Vol 2, No. 2, April 2011
- B.General Test, (2001) Atomic absorption spectrophotometry, Retrieved December 2011, 2011 from [http://www.ffcr.or.jp/zaidan/FFCRHOME.nsf/7bd44c20b0dc562649256502001b65e9/146fd852cd5e269049256f32001a133e/\\$FILE/B03.pdf](http://www.ffcr.or.jp/zaidan/FFCRHOME.nsf/7bd44c20b0dc562649256502001b65e9/146fd852cd5e269049256f32001a133e/$FILE/B03.pdf)
- Chen, C., and Wang, X (2006). Adsorption of Ni(II) from aqueous solution using oxidized multiwall carbon nanotubes, *Ind. Eng. Chem. Res.* 2006, 45, 9144-9149.
- Ebrahimpour, M., and Mushrifah, I. (2007). Heavy metal concentrations in water and sediments in Tasik Chini, a freshwater lake, Malaysia. *Environ Monit Assess* (2008) 141:297-307
- Fulazzaky, M. A., Seong, T. S., and Masirin, M. I. M. (2009). Assessment of water quality status for the Selangot River in Malaysia. *Water Air Soil Pollut* (2010) 205:63-77
- Gupta V. K., Rastogi A. and Nayak A. (2010). Adsorption studies on the removal of hexavalent chromium from aqueous solution using a low cost fertilizer industry was material, *Journal of Colloid and Interface Science* 342 (2010) 135-141

- Klein K.L., Malechko A.V., Mc Knight T.E., Retterer S.T, Rack P.D., Fowlkes J.D., Joy D.C and Simpson M.L. (2008) Surface characterization and functionalization of carbon nanofibers, *Journal of Applied Physics* 103, 16301 (2008)
- Korneva G. (2008) Functionalization of carbon nanotubes, *a PHD thesis submitted to Drexel University*
- Lee Y.G and Im Sun Im (2010) Preparation of functionalized nanofibers and their application, *Chungnam National University, Republic of Korea*
- Li, Y.H., Ding, J., Luan, Z., Di, Z., Zhu, Y., Xu, C., Wu, D., and Wei, B. (2003). Competitive adsorption of Pb^{2+} , Cu^{2+} , and Cd^{2+} ions from aqueous solutions by multiwalled carbon nanotubes, *Carbon* 41 (2003) 2787-2792.
- Lim, P. E., and Kiu, M. Y., (1994). Determination and speciation of heavy metals in sediments of the Juru River, Penang, Malaysia. *Environ. Monit Assess* (1995) 35: 85-95
- Lu, C and Chiu, H., (2007). Chemical modification of multiwalled carbon nanotubes for sorption of Zn^{2+} from aqueous solution, *Chemical Engineering Journal* 139 (2008) 462-468.
- Lu, C., Chiu, H., and Liu, C. (2006). Removal of Zn(II) from aqueous solution by purified carbon nanotubes: kinetics and equilibrium studies, *Ind. Eng. Chem. Res.* 2006, 45, 2850-2855
- Ma, G., Gonzalez, G. W., *Environmental Sampling & Monitoring Primer – Flame Atomic Absorption Spectrometry*. Retrieved December 2011, 2011 from <http://www.cce.vt.edu/ewr/environmental/teach/smprimer/aa/aa.html>
- Ominami Y., Ngo Q., Austin A.J., Yoong H., Yang C.Y., Cassell A. M., Cruden B. A., Li J., Meyyappan M., (2005)., Structural characteristics of carbon nanofibers for on-chip interconnect applications, *Appl.Phys. Lett.* 87 233105(2005);
- Parades J.I, Martinez-Alonso A., Tascon J.M.D. (2002). Oxygen plasma modification of submicron vapor grown carbon fibers as studied by scanning tunneling microscopy, *Carbon* 40 (2002) 1101-1108

- Rodriguez N.M, Terry R, Baker K (2000) Removal of heavy metals and organic contaminants from aqueous streams by novel filtration methods, *U.S Department of Energy, Final Report, Northeastern University*
- Ros T.G., Van Dillen A.J., Geus J.W., Koningsberger D.C. (2002) Surface of untreated parallel and fishbone carbon nanofibers: An infrared study *ChemPhysChem, Vol 3, Issue 2 209-214, 2002*
- Srivasta V. C., Mall I. D., Mishra I. M., (2007). Removal of cadmium(II) and zinc(II) metal ions from binary aqueous solution by rice husk ash, *Colloids and Surfaces A:Physicochem Eng. Aspects 312 (2008) 172-184*
- Stafiej, A. and Pyrzyńska, K.(2007). Adsorption of heavy metal ions with carbon nanotubes, *Separation and Purification Technology 58(2007)49-52.*
- Wang, S.H., Gong, W.X., Liu, X.W., Yao, Y.W, Gao, B.Y and Yue, Q.Y (2007). Removal of lead(II) from aqueous solution by adsorption onto manganese oxide coated nanotubes, *Separation and Purification Technology, 58(2007)17-23.*
- Xia W., Su. D., Birkner A., Ruppel L., Wang Y., Woell C., Qian Jun., Liang C., Marginean G., Brandl W., and Muhler M. (2005) Chemical vapour deposition and synthesis on carbon nanofibers: Sintering of ferrocene-derived supported iron nanoparticles and the catalytic growth of secondary carbon nanofibers, *Chem. Mater 2005, 17, 5737-5742*

APPENDICES

APPENDIX A

Findings of previous researches on metal adsorption using various types of adsorbents

Author	Year	Title	Objective	Findings					
				Metal ion	Adsorbent & surface area	Condition	Adsorption uptake	Parameters	Conclusion
Mumtaz Ali Atieh	2011	Effect of functionalized carbon nanofibers with carboxylic function group on the removal of zinc from water	To remove zinc using CNFs with raw CNFs R-CNFs and carboxylic functional group CNFs (M-CNFs) and to study the effect of pH, contact time, zinc concentration, CNFs dosage and agitation speed	Zinc(II)	CNFs purchased from Nanostructured & Amorphous Materials, Inc, USA, outside diameters 100-200nm, added with 300ml of concentrated nitric acid for 2g as-received CNFs. Cooled and diluted with 500 ml deionised water	Contact time: 2 hr Speed: 150 rpm Dosage of CNFs: 50g pH: 7	At pH 4, 20% removal of zinc by raw CNF, 90% of removal by modified CNFs 220 minutes of contact time contribute to >90% removal using M-CNFs and around 30% using R-CNFs At 50mg CNFs, >95% metal removal using M-CNFs, <20% removal using R-CNFs Removal of metal optimum at 150 rpm for M-CNFs (80-90% removal) while for R-CNFs optimum at 200rpm (20-30% removal)	pH : 4-7 Contact time : 10 – 220 minutes CNFs dosage: 50-150 mg Speed: 50-200 rpm Zinc concentration: 1, 1.5, 2 ppm	Percentage uptake increased with increase in pH, slightly increase with increase in agitation speed, optimal at higher dosage of CNFs, Low concentration of zinc CNFs with carboxylic functional group is better

							1 ppm zinc will give highest removal using M.CNFs (80-90% removal) while 1.5 ppm zinc give highest removal for R-CNFs (20-30% removal)		than raw CNFs.
Yehya M. Ahmad, Abdullah Al-Mamun, S.A Muyibi, Ma'anFahm i R. Al-Khatib, A.T Jameel and Mohammed A. Alsaadi	2010	Study of Pb adsorption by carbon nanofibers grown on powdered activated carbon	To remove Pb(II) from the aqueous solution using CNFs from palm kernel shell granular activated carbon	Pb(II)	CNFs derived from palm kernel shell granular activated carbon (obtained from Effigen Carbon (M) SdnBhd)	Contact time: 2 hr Speed: 150 rpm	Optimum metal removal was obtained at pH 5.5 and remained constant at higher pH Specific metal uptake increased with an increase in the sorbate concentration. The highest uptake of CNFs was around 89 mg g ⁻¹ at the initial Pb concentration of 70 mg L ⁻¹ with lowest sorption capacity of 15.88 (mg g ⁻¹) at initial concentration of 5 mg L ⁻¹ .	pH of lead solution from 2 to 10.5 Metal solution of varying concentrations of lead ranging from 5-70 mg L ⁻¹	Increase in pH (until 5.5) increase sorption capacity Sorption capacity increases with increase initial concentration.
S. A Sharma, M.A Gad	2010	Removal of heavy metals (Fe ³⁺ , Cu ²⁺ , Zn ²⁺ , Pb ²⁺ , Cr ³⁺ and Cd ²⁺) from aqueous solutions by using hebba clay and activated carbon	To investigate the adsorption capacity of hebba clay and activated carbon towards (Fe ³⁺ , Cu ²⁺ , Zn ²⁺ , Pb ²⁺ , Cr ³⁺ and Cd ²⁺) metals ion	Fe ³⁺ , Cu ²⁺ , Zn ²⁺ , Pb ²⁺ , Cr ³⁺ and Cd ²⁺	Hebba clay and activated carbon	Contact time: 4 hours Speed: 100 rpm	Using Hebba clay- Maximum removal was obtained for Fe ³⁺ ion, which nearly equal to 99.99%, the removal percentage increased as the weight of sorbent used increased., Minimum removal was obtained for Pb ²⁺ ion, but slightly increased by the increase in the weight of sorbent clay. The removal of Cd ²⁺ is slightly increased by the increase in the weight of sorbent	Adsorbent used (hebba clay): (0.1, 0.2, 0.3 and 0.4 gm) Contact timeL 2, 4 and 8 hrs pH: 2.06, 3.77 and 4.86 initial heavy	The removal of heavy metals ions was pH dependent, as the adsorption capacity increase with increasing pH value of solution, and at a particular pH , the order of

								metals concentration: (5,10, 30 and 50 mg/L)	increasing removal percentage was $Pb^{2+} < Cu^{2+} < Cd^{2+} < Cr^{3+} < Zn^{2+} < Fe^{3+}$ for hebba clay and $Cd^{2+} < Zn^{2+} < Cu^{2+} < Pb^{2+} < Cr^{3+} < Fe^{3+}$
Shu-Guang Wang, Wen-Xin Gong, Xian-Wei Liu, Ya-Wei Yao, Bao-Yu Gao, Qin-Yan Yue	2007	Removal of lead(II) from aqueous solution by adsorption onto manganese oxide-coated carbon nanotubes	To remove Pb(II) from the aqueous solution using Mn oxide-coated nanotubes ($MnO_2/CNTs$)	Pb(II)	$MnO_2/CNTs$ – Mn oxide was coated on the CNTs surface through a redox process	Contact time: 2 hr Temperature: 25°C	$MnO_2/CNTs$ is better adsorbent than pristine CNTs Adsorption increased from 57-81 mg/g with increasing MnO_2 load from 10-30% Metal removal varied from 77-98% with a change in pH from 2-4	Type of adsorbents: raw and modified CNTs MnO_2 load pH: 2-7	The optimum MnO_2 loading is 30% wt
Anna Stafiej and Krystyna Pyrzynska	2007	Adsorption of heavy metal ions with carbon nanotubes	To study the adsorption characteristic of some divalent metal ions (Cu, Co, Cd, Zn, Mn and Pb)	Cu(II), Co(II), Cd(II), Zn(II), Mn(II), and Pb(II)	Multiwalled carbon nanotubes (produced by catalytic vapour decomposition) purchased from Aldrich with 5-10 nm in outer diameter, surface area of 40-	pH: 9 Contact time: 4 hr	Adsorption increases with increasing pH 3-9 (Mn is the lowest while Cu is the highest)	pH: 3-9	$Cu(II) > Pb(II) > Co(II) > Zn(II) > Mn(II)$ Increased in adsorption by increasing pH

					600m ² /g and purity > 95%				
Chungsyng Lu Huantsung Chiu	2007	Chemical modification of multiwalled carbon nanotubes for sorption of Zn ²⁺ from aqueous solution	To identify the best modification for Zinc(II) removal and to study their characterization and isotherm of Zn(II) in an aqueous solution	Zn(II)	Multiwalled carbon nanotubes (MWCNTs) with outer diameter =< 10nm oxidized by mixed HCl, HNO ₃ /H ₂ SO ₄ (3N+1S), HNO ₃ , KmnO ₄ and NaClO	Bath shaker speed: 180 rpm Temperature: 25°C Contact time: 12h	At equilibrium with c ₀ : 30 mg L ⁻¹ 2.72 mg g ⁻¹ for MWCNTs(HCl) 3.52 mg g ⁻¹ for MWCNTs(H ₂ SO ₄) 5.01 mg g ⁻¹ for MWCNTs(H ₂ O ₂) 7.03 mg g ⁻¹ for MWCNTs(O ₃) 13.6 mg g ⁻¹ for MWCNTs(3N+1S) 18.48 mg g ⁻¹ for MWCNTs(HNO ₃) 21.61 mg g ⁻¹ for MWCNTs(KmnO ₄) 25.52 mg g ⁻¹ for MWCNTs(NaClO)	Oxidizer: HCl, H ₂ SO ₄ , H ₂ O ₂ /HNO ₃ /H ₂ SO ₄ (3N+1S), HNO ₃ , KmnO ₄ and NaClO	Physicochemical properties of MWCNTs were improved after oxidization – possess a better sorption performance. MWCNTs(NaClO) is the most effective sorbents
Chungsyng Lu, Huantsung Chiu, and Chunti Liu	2006	Removal of Zinc(II) from aqueous solution by purified carbon nanotubes: Kinetics and equilibrium	To remove Zn(II) from the aqueous solution using single-walled carbon nanotubes (SWCNTs) and multiwalled	Zn(II)	SWCNTs with dp< 2nm (L-type, Nanotech Port Co., Shenzhen, China) and commercially available MWCNTs	Bath shaker condition: 180 rpm Contact time: 12 hr	Sorption of Zn(II) increased quickly with time and then slowly reached equilibrium at 60 without regard to temperature As temperature increased from 5 – 45 °C, max. Zn(II) sorption of SWCNTs and MWCNTs calculated by Langmuir increased from 37.03 to	T: 5,15,25,35 and 45 °C	Sorption capacity of SWCNTs is greater than MWCNTs. As temperature increased from 5 – 45 °C, sorption

		studies	carbon nanotubes (MWCNTs)				46.94 mg/g and from 30.3 to 34.36 mg/g		capacity increased
Changlun Chen and Xiangke Wang	2006	Adsorption of Ni(II) from aqueous solution using oxidized multiwall carbon nanotubes	To remove Ni(II) using multiwall carbon nanotubes (MWCNTs) as novel adsorbent	Ni(II)	MWCNTs, using N ₂ -BET method, the surface area of the free, dried oxidized MWCNTs/HNO ₃ was 197m ² g ⁻¹	T: 291±1K Bath shaker speed: 300 rpm pH: 6.55±0.02 Contact time: 24 hr	The equilibrium was reached within 40 min for all concentrations Increase in uptake capacity with increasing MWCNTs conc. (oxidized MWCNTs is better than as-grown CNTs) Uptake optimum at pH 8. Distribution coefficient increase with a rise in temperature	MWCNTs conc: 0.25m/V – 1.0 m/V Contact time: 0 – 300 minutes T: 291±1, 303±1, 313±1, and 333±1 K pH: 3.5 – 8.5	Oxidized MWCNTs has great potential of removing metal ions from aqueous solution
Yan-Hui Li, Jun Ding, Zhaokun Luan, Zechao Di, Yuefeng Zhu, CailuXu, Dehai Wu, Bingqing Wei	2003	Competitive adsorption of Pb ²⁺ , Cu ²⁺ , and Cd ²⁺ ions from aqueous solutions by multiwall carbon nanotubes	To remove Pb(II), Cu(II), and Cd(II) by nitric acid treated multiwall carbon nanotubes (MWCNTs)	Pb(II), Cu(II) and Cd(II)	Nitric acid treated MWCNTs	pH: 5 Contact time: 4 hr	Adsorption of metals maximum at pH 6-8 Increased in MWCNTs dosage increasing the adsorption percentage	pH: 2.3 -11.0 CNTs dosage: 0.05 – 0.3 g treated MWCNTs to 100ml solution	Adsorption affinity Pb(II) >Cu(II) > Cd(II) Competitive adsorption capacity increased with increasing pH and MWCNTs dosage

APPENDIX B

Effect of contact time and initial concentration on lead adsorption

Design conc	Initial (ppm)	Time (hour)	Final (ppm)	%Ads.	mg/g
5	5.6627	0	5.6627	0.000	0
5	5.6627	0.33	0.2943	94.803	5.3684
5	5.6627	1	0.382	93.254	5.2807
5	5.6627	1	0.288	94.914	5.3747
5	5.6627	2	0	100.000	5.6627
5	5.6627	4	0.2254	96.020	5.4373
5	5.6627	6	0.025	99.559	5.6377
5	5.6627	24	1.7846	68.485	3.8781
10	8.0987	0	8.0987	0.000	0
10	8.0987	0.33	2.4296	70.000	5.6691
10	8.0987	1	4.4083	0.000	3.6904
10	8.0987	1	0.0376	99.536	8.0611
10	8.0987	2	4.4584	44.949	3.6403
10	8.0987	4	4.4458	45.105	3.6529
10	8.0987	6	0.025	99.691	8.0737
10	8.0987	24	0.0125	99.846	8.0862
15	8.6472	0	8.6472	0.000	0
15	8.6472	0.33	1.1396	86.821	7.5076
15	8.6472	1	0.0751	99.132	8.5721
15	8.6472	1	3.9324	54.524	4.7148
15	8.6472	2	0	100.000	8.6472
15	8.6472	4	0	100.000	8.6472
15	8.6472	6	0	100.000	8.6472
15	8.6472	24	5.6731	34.394	2.9741
20	19.3742	0	19.3742	0.000	0
20	19.3742	0.33	2.7113	86.006	16.6629
20	19.3742	1	1.5028	92.243	17.8714
20	19.3742	1	2.3231	88.009	17.0511
20	19.3742	2	1.8785	90.304	17.4957
20	19.3742	4	2.2542	88.365	17.12
20	19.3742	6	2.2668	88.300	17.1074
20	19.3742	24.00	6.9192	64.287	12.455
25	22.0951	0	22.0951	0.000	0
25	22.0951	0.33	4.7339	78.575	17.3612
25	22.0951	1	5.1221	76.818	16.973
25	22.0951	1	7.5955	65.624	14.4996
25	22.0951	2	0.8892	95.976	21.2059
25	22.0951	4	0.6011	97.279	21.494
25	22.0951	6	0	100.000	22.0951
25	22.0951	24	10.4008	52.927	11.6943

APPENDIX C

Effect of contact time and initial concentration on chromium adsorption

Designed conc	Initial (ppm)	Time (hour)	Final (ppm)	%Ads.	mg/g
5	0.1658	0	0.1658	0	0
5	0.1658	0.33	0.0704	57.53920386	0.0954
5	0.1658	0.67	0.0414	75.03015682	0.1244
5	0.1658	1	0.058	65.01809409	0.1078
5	0.1658	2	0.058	65.01809409	0.1078
5	0.1658	4	0.0373	77.50301568	0.1285
5	0.1658	6	0.0041	97.52714113	0.1617
5	0.1658	24	0.0124	92.52110977	0.1534
10	0.9779	0	0.9779	0	0
10	0.9779	0.33	0.3149	67.79834339	0.663
10	0.9779	0.67	0.0414	95.76643829	0.9365
10	0.9779	1	0.0249	97.45372737	0.953
10	0.9779	2	0.0249	97.45372737	0.953
10	0.9779	4	0.0166	98.30248492	0.9613
10	0.9779	6	0.0249	97.45372737	0.953
10	0.9779	24	0.0249	97.45372737	0.953
15	1.6493	0	1.6493	0	0
15	1.6493	0.33	0.0497	96.98660038	1.5996
15	1.6493	0.67	0.0746	95.47686897	1.5747
15	1.6493	1	0.0249	98.4902686	1.6244
15	1.6493	2	0.0166	98.9935124	1.6327
15	1.6493	4	0.058	96.48335658	1.5913
15	1.6493	6	0.0663	95.98011278	1.583
15	1.6493	24	0.0497	96.98660038	1.5996
20	2.3454	0	2.3454	0	0
20	2.3454	0.33	0.0497	97.88095847	2.2957
20	2.3454	0.67	0.0663	97.17319007	2.2791
20	2.3454	1	0.1575	93.28472755	2.1879
20	2.3454	2	0.0912	96.11153748	2.2542
20	2.3454	4	0.1036	95.58284301	2.2418
20	2.3454	6	0.0083	99.6461158	2.3371
20	2.3454	24.00	0.0249	98.9383474	2.3205
25	3.2985	0	3.2985	0	0
25	3.2985	0.33	0.0166	99.49674094	3.2819
25	3.2985	0.67	0.116	96.48324996	3.1825
25	3.2985	1	0.1243	96.23162043	3.1742
25	3.2985	2	0.0995	96.98347754	3.169
25	3.2985	4	0.0912	97.23510687	3.2073
25	3.2985	6	0.0746	97.73836592	3.2239
25	3.2985	24	0.058	98.24162498	3.2405

APPENDIX D

Effect of temperature on lead adsorption

conc	T	Initial (ppm)	Time (hour)	Final (ppm)	%Ads.	mg/g
25	25	22.0951		0.0626	99.71668	22.0325
25	35	22.0951	24	1.5341	93.05683	20.561
25	45	22.0951		3.8948	82.37256	18.2003

Effect of temperature on chromium adsorption

conc	T	Initial (ppm)	Time (hour)	Final (ppm)	%Ads.	mg/g
25	25	3.2985		0.0249	99.24811	3.2736
25	35	3.2985	24	0.058	98.24162	3.2405
25	45	3.2985		0.0041	99.8757	3.2944

APPENDIX E

Effect of pH on lead adsorption

conc	Ph	Initial (ppm)	Time (hour)	Final (ppm)	%Ads.	mg/g
25	1	22.0951	24	5.3881	75.62763	16.71
25	3	22.0951	24	1.2023	94.55852	20.8928
25	5	22.0951	24	18.4972	16.2837	3.5979
25	6	22.0951	24	0.0626	99.71668	22.0325
25	7	22.0951	24	8.516	61.45752	13.5791
25	9	22.0951	24	0	100	22.0951
25	11	22.0951	24	9.5679	56.69673	12.5272
25	12.36	22.0951	24	21.206	4.023969	0.8891

Effect of pH on chromium adsorption

conc	Ph	Initial (ppm)	Time (hour)	Final (ppm)	%Ads.	mg/g
25	1	3.2985	24	2.4036	27.13051	0.8949
25	3	3.2985	24	2.3731	28.05518	0.9254
25	5	3.2985	24	0.0622	98.11429	3.2363
25	6	3.2985	24	0.0249	99.24511	3.2736
25	7	3.2985	24	0.0207	99.37244	3.2778
25	9	3.2985	24	0.0249	99.24511	3.2736
25	11	3.2985	24	0.2279	93.0908	3.0706
25	12.4	3.2985	24	1.5249	53.7699	1.7736
25	12.58	3.2985	24	0.058	98.24162	3.2405